



euHeart

Personalised & Integrated Cardiac Care: Patient-specific Cardiovascular Modelling and Simulation for In Silico Disease Understanding & Management and for Medical Device Evaluation & Optimization

FP7-ICT-2007

IP Contract no: 224495

Project Final Report

Start date of project: 01 June 2008

Duration: 54 months

Revision 1.0 (10th April 2013)

Project coordinator:	J. Weese
Scientific coordinator:	N. Smith
Clinical coordinator:	R. Razavi
WP leaders:	D. Chapelle H. Delingette A. Frangi R. Hose P. Hunter J. Spaan

Table of Contents

1. Executive Summary	4
2. Context and Objectives of the euHeart Project	6
3. WP1 - Integrated Multi-Scale Cardiac Modeling	9
3.1. Anatomical Models Database (AMDB)	9
3.2. Establishment of Functional Community Benchmarks	10
3.3. Heart Gen service for generating computational cardiac meshes	10
3.4. Use of AMDB to identify anatomical changes	11
4. WP2 – Modeling Standards and Software Tools	12
4.1. Scope of CellML and FieldML	12
4.2. CellML models	13
4.3. FieldML version 0.5	13
4.4. Model visualization	15
5. WP3 - Anatomical Model Personalization	16
5.1. Anatomical models with scar	16
5.2. Vessel segmentation	17
5.3. Motion estimation	18
5.4. Aorta segmentation with pressure constraint	18
6. WP4 – Biophysical Model Personalization	20
6.1. Verdandi data assimilation library	20
6.2. Training and expertise transfer	21
6.3. Proofs of concept studies	22
7. WP5 – Cardiac Resynchronization Therapy	25
7.1. CRT Planning environment	25
7.2. New indices for patient selection	26
7.3. Simulation-based prediction of CRT treatment response	27
8. WP6 – Cardiac Radiofrequency Ablation	28
8.1. Atrial fiber architecture	28
8.2. Prediction of outcome of RFA redo procedures	29
8.3. Personalization of EP models from ventricular endocardial mapping	29
8.4. Prediction of VT re-entry patterns	31
8.5. ECGI during VT Stim	32
9. WP7: Heart Failure	33
9.1. Fluid-Structure models for simulating LVAD cardiac function	33
9.2. Optimal LVAD flow regimes for promoting cardiac remodeling	35
9.3. Anatomy and diastolic filling in systemic right ventricular patients	35
9.4. Novel metric for characterizing systemic right ventricular patients	36
10. WP8 – Coronary Artery Disease	37
10.1. Coronary microvascular structure	38
10.2. Multiscale multiphysics model for coronary perfusion	38
10.3. Clinical MRI perfusion and coronary hemodynamics	39
10.4. Validation of MRI perfusion measurements	41
10.5. Model for whole heart perfusion	41
11. WP9 - Valvular and Aortic Disease	42
11.1. Circulation and anatomical models for public access	43
11.2. Work flows for aortic and valvular disease	43
11.3. Evaluation of work flows in clinical centers	46
12. WP 10 – Clinical Data Acquisition and Validation	48

12.1. Free breathing cardiac MRI with advanced motion compensation	48
12.2. Highly accelerated and accurate MR flow.....	49
12.3. Flow quantification from 3D Doppler ultrasound	50
12.4. Curvilinear analysis and approximation of cardiac DTI <i>in-vivo</i>	50
12.5. Endovascular simulator for radiofrequency ablation	51
13. Conclusions.....	53
14. Impact	55
14.1 Contribution to better healthcare	55
14.2 Medical device innovation.....	56
14.3 Contribution to the VPH	56
15. Contact Information	58

1. Executive Summary

Heart disease represents a highly relevant and epidemiologically significant contributor to loss of quality and quantity of life within Europe. This, currently western, epidemic is now also spreading to developing nations. Early detection and prediction of the progression of CVD are key requirements towards improved treatment, a reduction in mortality and morbidity, and of course to reduce healthcare costs within the European economy. The euHeart project focused on the development of methods for the patient-specific modeling of the heart's anatomy and physiology with a focus on 5 important disease respective treatment areas: cardiac resynchronization therapy, radiofrequency ablation, heart failure, coronary artery disease and aortic and valvular disease. Its specific objective was to improve diagnosis, treatment planning and delivery, and optimization of implantable devices by making cardiac models patient-specific.

The euHeart project built on the previous generation of advanced cardiac models and used state-of-the-art clinical imaging to develop new and personalized models of individual cardiac physiology. To fully exploit the expertise in the consortium and enable sharing of the results with the wider VPH community, a web-based database has been developed, populated with models, and extended with computing services facilitating model building. The modeling standards CellML and FieldML have been advanced to make models and simulation approaches sustainable as other groups can reuse and build upon previous results. Methods have been developed that allow for the efficient generation of patient-specific anatomical models from medical images of multiple imaging modalities. In addition, a framework for the assimilation of model parameters has been developed that assimilates observations into a model by acting on the discrepancy between the measurements and the values derived from the computational model.

Adaptation of the models and simulation approaches for the 5 disease areas resulted in a wealth of new approaches, technical improvements and insights. The models, simulations and prototypes built upon the models were focused on clinical questions in relation to the 5 disease areas. To provide data for model development, to show the benefit of the developed models and to quantify their clinical benefit, the work in euHeart was accompanied by clinical data acquisition activities. These data allowed demonstrating that, for instance, a personalized electromechanical model of the left and right ventricular myocardium is able to predict the acute response to CRT for two patient cases. Models and simulations have also been used to derive new clinical indices.

Proven by more than 300 publications of which 128 have been published in peer-reviewed journals, the euHeart project significantly advanced the state-of-the-art in cardiac simulations. The project demonstrated the predictive value and clinical potential of personalized cardiac simulations for several clinically relevant settings. Setting up personalized models and simulations was very time consuming limiting validation to a small number of patient cases. Clinical

validation for a large number of patient cases is intended to be done in future projects.

The impact of the euHeart project is threefold. First, the results allow improving healthcare in the area of heart disease that is a highly relevant and epidemiologically significant contributor to loss of quality and quantity of life within Europe. Second, the results allow innovating medical devices. Finally, the euHeart made a significant contribution to the VPH community and vision.

2. Context and Objectives of the euHeart Project

The euHeart project was a European research initiative targeting the personalized diagnosis and treatment of cardiovascular disease. The project combined seventeen industrial, clinical and academic partners including Philips Research and Philips Healthcare. The project duration was 54 months with a budget of 19.05 million.

Heart disease represents a highly relevant and epidemiologically significant contributor to loss of quality and quantity of life within Europe. Cardio-vascular disease (CVD) causes over 4.35 million deaths including nearly half of all non-accidental deaths (Petersen, S., et al., European cardiovascular disease statistics, 2005 edition). This, currently western, epidemic is now also spreading to developing nations, and was predicted to become the most common cause of death in these countries by 2010 (The World Health Organization (WHO), <http://www.who.int>, 2003). CVD manifests itself in diseases such as coronary artery disease, congestive heart failure, and cardiac arrhythmias. These diseases have a significant impact on the EU economy with an estimated cost of EUR 169 billion a year (Petersen, S., et al., European cardiovascular disease statistics, 2005 edition). This significant financial burden is spread across community sectors with approximately 62% of costs due to direct health care costs, 21% due to productivity losses and 17% due to the informal care of people with CVD. Thus the early detection and prediction of the progression of CVD are key requirements towards improved treatment, a reduction in mortality and morbidity, and of course to reduce healthcare costs within the European economy.

Describing human anatomy, physiology and disease and predicting its behavior from patient-specific measurements is the ambitious goal of the wider Virtual Physiological Human (VPH) initiative. The euHeart project focused on the development of methods for the patient-specific modeling of the heart and its major diseases. Its specific objective is to improve diagnosis, treatment planning and delivery, and optimization of implantable devices by making cardiac models patient-specific using clinical measurements. To achieve this goal, euHeart built on the previous generation of advanced cardiac models (Hunter, P., et al., *Mech Ageing Dev*, 2005. 126(1): 187-92, Smith, N., et al., *J Exp Biol*, 2007. 210: 1576-1583) and used state-of-the-art clinical imaging to develop new and personalized models of individual cardiac physiology. The goal of this approach was not only to improve the understanding of cardiovascular disease (CVD) but more importantly to demonstrate the potential of biophysical models for significantly improving healthcare.

The specific cardiovascular diseases on which the euHeart project focused are:

- Congestive heart failure, either due to abnormal activation (treated with cardiac resynchronization therapy) or due to structural abnormalities ((corrected) congenital heart disease) leading to abnormal hemodynamic and loading (treated by ventricular assist devices, potentially as a bridge to transplantation).

- Cardiac arrhythmias, arising from congenital defects or structural abnormalities induced by coronary artery disease and hypertension, and resulting in symptoms and increased risk of sudden death (treated by radiofrequency ablation).
- Abnormal myocardial tissue perfusion in coronary artery disease, potentially in the absence of a significant epicardial vessel stenosis or after percutaneous interventions.
- Abnormalities in hemodynamic and loading due to valvular or aortic disease, resulting in inefficient cardiac dynamics and with high risk of future remodeling and heart failure.

The approach followed in the euHeart project is to divide the work packages (WPs) into two groups: the technical and application WPs (see Figure 1). The technical WPs (WP1-4) developed common technology and concentrated their efforts on the development of *generic* tools including databasing and model benchmarking (WP1), modeling standards and visualization tools (WP2), multi-modal image analysis (WP3), and assimilation techniques to personalize simulation parameters (WP4). The application WPs (WP5-9) focused their activities on disease-specific developments such as the development and extension of biophysical models, acquisition and processing of biomedical data, integration into prototypes, and validation for Cardiac Resynchronization Therapy (WP5), Radiofrequency Ablation (WP6), Heart Failure (WP7), coronary artery disease (WP8) and valve & aortic disease (WP9). In addition, they defined the requirements for the development of research tools in the technical WPs. The structure was complemented by a workpackage on clinical data acquisition (WP10) and obligatory workpackages for handling dissemination and exploitation of knowledge and project:

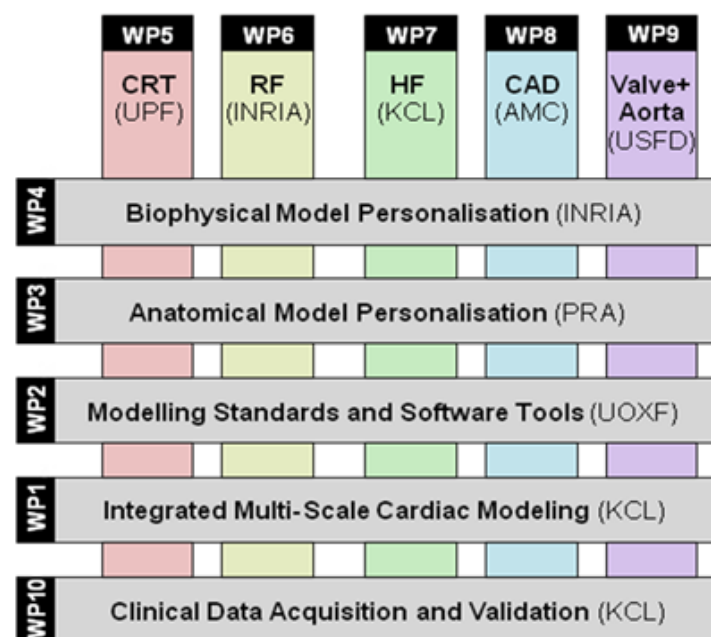


Figure 1 Diagram illustrating the euHeart workpackage structure. The technical workpackages WP1-WP4 develop common technology. The application workpackages WP5-WP9 focus on disease-specific developments. WP10 handles clinical data acquisition for model building and validation.

The project was carried out in a consortium with 16 partners from 6 countries comprising participants from industry, academia and clinics (see Section 14.3).

3. WP1 - Integrated Multi-Scale Cardiac Modeling

The objective of this work package was to provide a framework for applying biophysically based modeling principles and community standards that allows disseminating model development and research advances across the consortium and with the wider VPH community. The web-enabled database established in this work package has provided both the initial model and final repository for the model development cycle. The AMDB database is also used to make community benchmarks that enable robust verification of individual simulation codes publicly available. To assist with model creation, AMDB was complemented by the Heart Gen service for personalizing computational cardiac meshes. As an exemplary application, the AMDB infrastructure was used to investigate the impact of preterm birth on left ventricular structure and function in humans.

3.1. Anatomical Models Database (AMDB)

Sharing and reusing anatomical models (see Figure 2 for examples) over the Web offers a significant opportunity to progress the investigation of cardiovascular diseases. However, the previous sharing methodologies suffered from the limitations of static model delivery (i.e. embedding static links to the models within Web pages) and of a disaggregated view of the model metadata produced by publications and cardiac simulations in isolation. In the context of euHeart we have overcome the above limitations with the introduction of AMDB, a Web-enabled database for anatomical models of the heart. The database implements a dynamic sharing methodology by managing data access and by tracing all applications. In addition to this, AMDB establishes a knowledge link with the physiome model repository by linking geometries to CellML models embedded in the simulation of cardiac behavior. Furthermore, AMDB uses a version of the interoperable FieldML data format to effectively promote reuse of anatomical models, and incorporates a rendering engine, to provide three-dimensional graphical views of the models populating the database. Currently, AMDB stores 196 cardiac geometries and functional models developed within the euHeart project consortium.

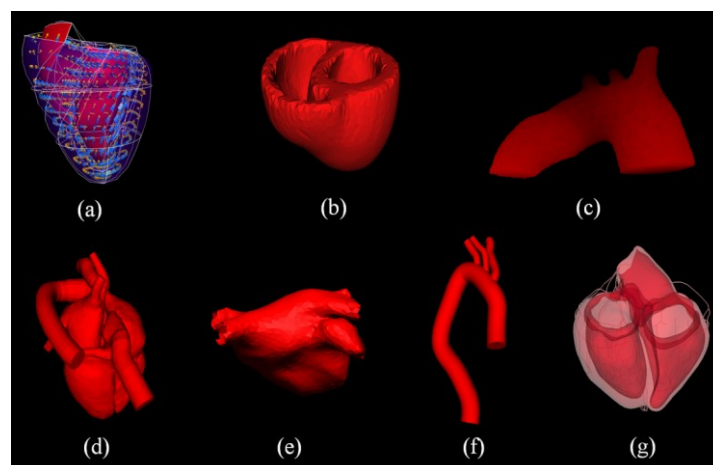


Figure 2 Three-dimensional visualizations of Auckland Heart (a), INRIA Heart (b), INRIA Aorta (c), Philips Cardiac Atlas (d), Philips Left Atrium (e), Sheffield Aorta (f) and UPF Heart (g).

3.2. Establishment of Functional Community Benchmarks

Simulations of electrical activation have advanced from analyzing emergent phenomena in simplified systems to detailed representations of physiology and pathologies within the heart. The large and active community focused on this work within both the euHeart and wider VPH projects has meant that these simulation frameworks have progressed to the point where they provide some of the most advanced current exemplars of multi-scale whole organ models. While this work continues to produce a large number of important scientific contributions, challenges are now emerging for the community in general. Specifically the increase in application domains has been paralleled by growth in the number of software packages available to perform these simulations and the complexity of the enabling methods. This situation is now, in turn, impeding the ability to review and, in some cases, reproduce simulation results. For cardiac electrophysiology simulation software this is challenging for authors to address, given that in contrast to the field of fluid and solid mechanics, there are no analytic solutions or community agreed benchmark problems to compare the code output against.

Thus motivated by the exemplar status, increased complexity and clinical application of euHeart cardiac models, we established community benchmarks that enable robust verification of individual simulation codes and a discussion of benchmarking in general within the VPH community. Results of this benchmark problem are reported on from 10 independent software platforms at 9 combinations of spatial and temporal resolution. This provides a library of simulation results that allows new codes and numerical methods to be evaluated against. The results are published online on the publically assessable AMDB database. Using this database results from these 90 benchmark simulations can be interactively compared and new results submitted.

3.3. Heart Gen service for generating computational cardiac meshes

AMDB addresses the questions of sharing data amongst scientists and clinicians, and it is a logical extension to also assist in the creation of cardiac models itself. In most cases cardiac and other anatomical models are created through various processes of converting imaging data into meshes, often manually and usually with the use of complex tool chains. Making this process simpler and more accessible has been addressed through the use of web services in collaboration with the VPH-Share project. By providing a mesh generation tool as an online service, we have eliminated the need to install software locally. The web interface provides control over the tool's use, and in general simplifies the process through which users interact with it. This new service is the HeartGen tool, implemented as a standard form of web service in AMDB. In particular, HeartGen allows to adapt the geometry of cardiac models to stacks of segmented images derived from 3D imaging modalities. The user interface front end is organized around a work-flow process allowing the user to perform the fitting process with a varying set of parameters until a satisfactory fitted model is produced. These generated models can then be stored in AMDB in the same manner as user-provided data, as well as being emailed to the user. Combining tools that do not need to be installed locally with the database

to store results remotely greatly simplifies and streamlines the process scientists must go through to create and disseminate data.

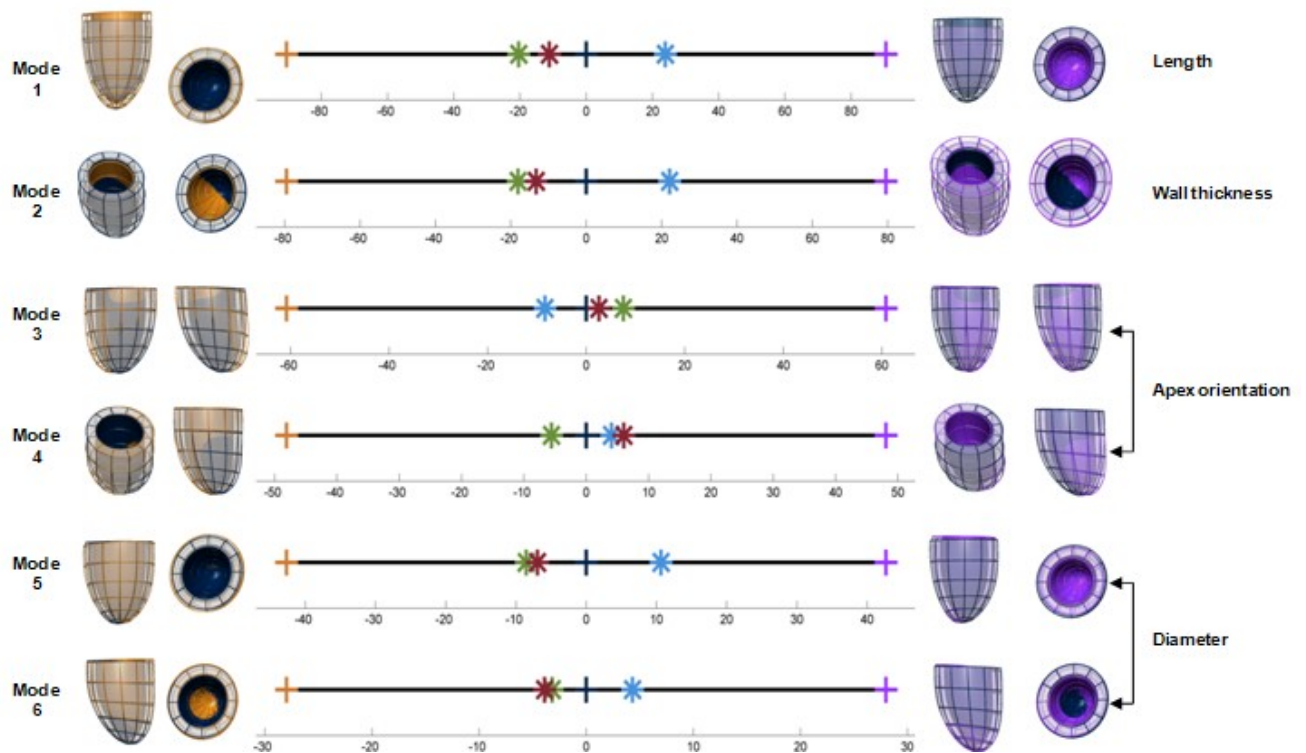


Figure 3 Comparison of shape differences between groups by modes of variation of the Principal Component Analysis. Comparison between groups was performed using a two-sided student T-test. The red line indicates $P=0.01$. The panel on the left shows a comparison of the preterm-born young adults and young adults born at term, demonstrating that the first six modes of variation differed significantly between groups.

3.4. Use of AMDB to identify anatomical changes

Using the AMDB infrastructure we have created a cardiac atlas to reveal for the first time the impact of preterm birth on left ventricular structure and function in humans. Furthermore, we investigated whether key pre- and post-natal factors associated with preterm birth, such as gestational age, exposure to preeclampsia, growth restriction, duration of postnatal ventilation or postnatal weight gain have additional impacts on the left ventricle relevant to adult cardiovascular health. Mesh models were derived from the binary masks representing the left ventricle of the individuals resulting in approximately 3000 nodal points per subject. Principal component analysis for the group as a whole was subsequently undertaken to identify key modes of variation. The left ventricular atlases have been made available for researchers to download at AMDB. From these results six modes of variation accounted for 84.2% of the variance in left ventricular geometry within the study population. Further analysis revealed that all six modes were significantly different between preterm and term-born groups (Figure 3). Visual assessment showed that preterm-born individuals had significantly shorter ventricles, increased left ventricular wall thickness, a reduced internal left ventricular cavity diameter, and a significant shift in apex orientation.

4. WP2 – Modeling Standards and Software Tools

Modeling standards are essential for exchanging complex computational models between different groups and for ensuring the enduring and far-reaching value of developed models and simulation approaches. The objective of WP2 was to develop and advance the modeling standards CellML and FieldML and to develop application programming interfaces (APIs) to facilitate the use of these standards – not only within the euHeart project, but also in future projects focusing on human organ systems others than the heart. In addition to the advances related to the modeling standards CellML and FieldML, the related open source software cmgui for visualizing models and simulation results has been enhanced. Furthermore, cmgui was integrated with the open source framework GIMIAS, a **workflow-oriented** environment for solving advanced biomedical image computing and individualized simulation problems.

4.1. Scope of CellML and FieldML

While scientists and mathematicians have invented many ingenious ways for making models and using computers to simulate these models, it has always been problematic to share these models with other researchers, or to transfer these effectively into clinical technologies for the treatment of patients. The problem is that, usually, very complex computer programs are used to construct the models in a way that focuses only on the original research goals, even though they have the potential to be used more broadly. If a modeling standard is used to share the model, a world of possibilities opens up. For example, the model becomes accessible to a broader community and the community can benefit by being able to use the model. In addition, the model can be further advanced and improved as the model becomes more widely used.

FieldML and CellML are the two modeling standards used in euHeart. CellML is a simpler standard, and is used to represent mathematical models that assume that quantities may vary with time, but do not vary spatially. Such models are useful when simulations must approximate complex cellular biochemistry. CellML is also capable of representing models that describe the mechanical properties of a particular type of substance or tissue, such as how the muscle fibre directions of the heart affect the stiffness. CellML was already a relatively mature standard at the start of the euHeart project, so the goal was to use CellML to represent significant cardiac cellular models and make them available to the consortium and the public via the internet.

FieldML allows the description of variations with respect to time and space, and in fact supports any number of independent variables. The quantities that vary are referred to as fields. This allows FieldML to represent the geometrical shape of a beating heart, as well as many other fields of interest in such a model, such as fields that represent the flow of blood through the chambers of the heart and the blood pressure variations at different locations and at different stages of the heartbeat. FieldML is very ambitious compared to CellML and its further development was an important goal of euHeart, aiming to at least achieve the ability to represent the majority of the time-varying spatial euHeart

models, and laying the foundation for future enhancements of both CellML and FieldML.

4.2. CellML models

Numerous CellML models were created for use in cardiac simulations (see Figure 4 for an example and Table 1 for a list). A key benefit of using CellML during euHeart was also that this provided feedback, which enabled the CellML software to be improved upon. The feedback has been taken into consideration for the design of the next CellML version. The work with CellML also served as groundwork for the more complex requirements of FieldML. For example, the CellML repository software development resulted in features that could be easily extended for initial FieldML support.

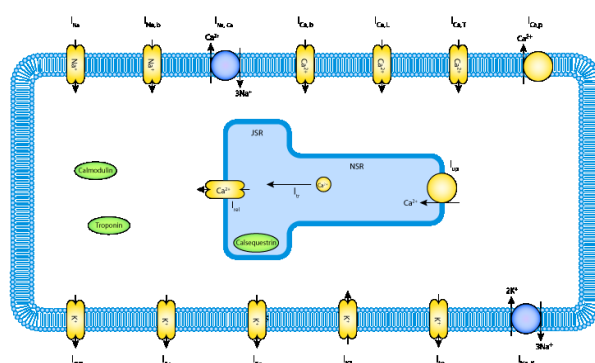


Figure 4 Schematic of a cellular scale lumped parameter CellML model (Aslanidi et al, 2009, available from <http://models.cellml.org/exposure/0e3a603db8f464ae89becb8d89225d90>)

- Pasek et al, 2008 (2 models: myocyte with cardiac transverse-axial T-system)
- Sachse, Moreno & Abildskov, 2008 (2 models: cardiac fibroblast)
- Aslanidi et al. 2009 (Atrial cell model)
- Aslanidi et al. 2009 (Purkinje model)
- Benson et al. 2008 (3 models - epicardial, endocardial and M cell)
- Decker et al. 2009 (epicardial cell)
- Inada et al. 2009 (3 models: Atrio-Nodal Cell, Nodal-His Cell, Nodal Cell)
- Maltsev & Lakatta 2009 (SA node cell)
- Stewart et al. 2009 (Purkinje fibre cells)
- Maltsev & Lakatta, 2009 (2 models: SA node cell)
- Tabak et al. 2010 & Tran et al. 2009 (models of the SERCA pump)
- Ohara et al 2011 (Human cardiac cell model)

Table 1 Some of the cardiac models made available in CellML (publically available at <http://models.cellml.org>).

4.3. FieldML version 0.5

Four new FieldML versions have been developed and released, the most recent of these being FieldML version 0.5. Table 2 provides a list of features supported by the different versions. With each of these versions of FieldML since version

0.2, a corresponding API was made available. Furthermore, significant progress has been made on the design for the next FieldML version.

Feature		Exnode Exelem	FieldML				
			v0.1	v0.2	v0.3	v0.4	v0.5
Technical	XML		✓	✓	✓	✓	✓
	Independent FieldML API			✓	✓	✓	✓
	External data sources					✓	✓
	Imports					✓	✓
	HDF5 support						✓
	Parallel I/O						✓
Model	1D elements	✓	✓	✓	✓	✓	✓
	2D Quadrilateral elements	✓	✓	✓	✓	✓	✓
	3D Hexahedral elements	✓	✓	✓	✓	✓	✓
	2D Simplex elements	✓	✓		✓	✓	✓
	3D Simplex elements	✓	✓			✓	✓
	Boolean evaluators						✓
	User defined tensor products of bases	✓	✓				
	Curvilinear coordinates	✓	✓				

Table 2 Features comparison of FieldML versions 0.1 through to 0.5.

The use of FieldML and the API for exchanging models was demonstrated by enabling two software packages – the open source visualization software cmgui and the open source simulation software OpenCMISS - to work with the FieldML format via the API. Using a simple example as a test, OpenCMISS read in parts of a model that were described using FieldML, ran the simulation, and then used FieldML to represent the simulation result. Cmgui was used to read in the FieldML representation of the simulation result and visualize it (Figure 5). The simulation itself was very simple, since the focus was on demonstrating the use of FieldML.

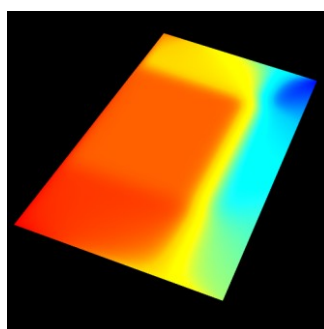


Figure 5 Cmgui visualization of the simple example used for testing FieldML 0.5 data exchange.

The model repository software that was initially used for making CellML models publicly available on the web was adapted to support FieldML models as well. This software is known as the PMR software (for Physiome Model Repository). For FieldML support, 3D visualization of models was enabled directly in the web browser, by means of the cmgui-Zinc web browser plugin.

4.4. Model visualization

Cmgui is an advanced 3D visualization software package with modeling capabilities. Cmgui is part of CMISS, a mathematical modeling environment initially developed by the University of Auckland Bioengineering Institute. Some of the main areas of functionality are:

- 3D visualization of finite element and boundary element meshes
- mesh creation
- mathematical field visualization and manipulation

The Zinc web-browser plug-in essentially enables the use of cmgui from JavaScript via the API, and embedded within HTML web pages. Figure 6 shows visualizations of some FieldML models and similar models.

As part of the euHeart project, cmgui was enhanced to support reading in a limited range of types of FieldML version 0.5 files, allowing validation of the use of FieldML for visualization. In addition, cmgui was integrated with GIMIAS allowing its use together with other GIMIAS plug-ins developed, for instance, for segmentation in workpackage WP3 to build a complete application. Figure 7 shows a screenshot of GIMIAS with a cmgui visualization in one of its viewports.

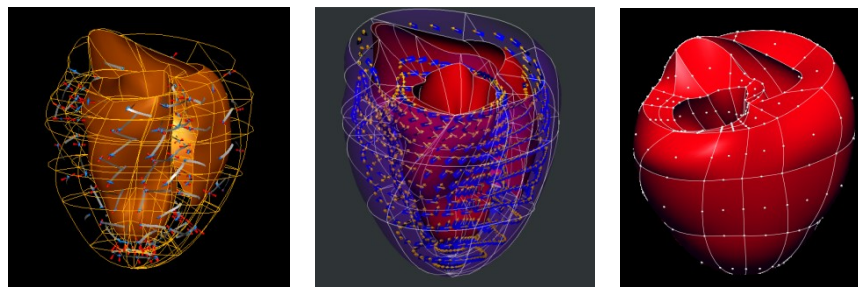


Figure 6 Visualizations of some FieldML models and similar models. The model on the right uses FieldML 0.5 features.



Figure 7 Screenshot of GIMIAS with a cmgui visualization (lower viewport).

5. WP3 - Anatomical Model Personalization

Workpackage WP3 focused on the development of generic image processing techniques that are required for VPH simulations of the heart and – according to the collected requirements - useful for multiple application packages. The resulting algorithms support the efficient or automatic segmentation of the heart including heart chambers, scar tissue in the myocardium and vascular structures such as the aorta, coronary arteries and coronary veins. In addition, algorithms for deriving motion and strain in the left ventricle from tagged MR sequences and 3D ultrasound sequences were developed. Finally, inclusion of biophysical constraints in image processing algorithms was investigated at the example of aorta segmentation. Most algorithms were integrated into GIMIAS to enable use by other consortium members and integration of the algorithms into larger application packages.

5.1. Anatomical models with scar

Personalized heart models generated by model-based segmentation from medical images lack usually certain characteristics that are essential for VPH simulations. For example, the myocardium is usually modeled by a single layer surface in most parts of the heart (Ecabert, O. et al., IEEE Trans Med Imag, 2008. 27(9): 1189-1201). This does not allow for modeling the dimension of the myocardium, and, hence, for representation of scar tissue distribution or a transmural signal propagation. We introduced, therefore, double-walled structures with a volumetric mesh between endo- and epicardium (8) and a mechanism to reconstruct the volumetric mesh after model adaptation.

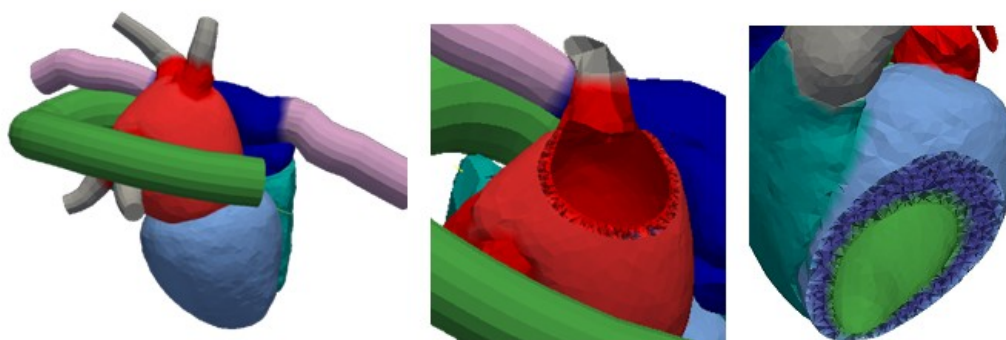


Figure 8 Mesh model of the heart (left). The left atrium (middle) and left ventricle (right) are represented by endo- and epicardial walls with volumetric meshes.

In addition, a processing chain was developed (see Figure 9) that allows constructing personalized heart models including the scar distribution in the left ventricle (LV). For that purpose an anatomical reference model with volumetric LV mesh is adapted to a 3D image like steady state free-precession (SSFP) MR scans. The resulting personalized heart shape is registered to late enhancement (LE) MR scans showing the scar distribution. By thresholding, it is decided for each tetrahedron of the volumetric LV mesh if it covers scar or healthy tissue. Alternatively, more refined classification methods may be used to distinguish scar from healthy tissue.

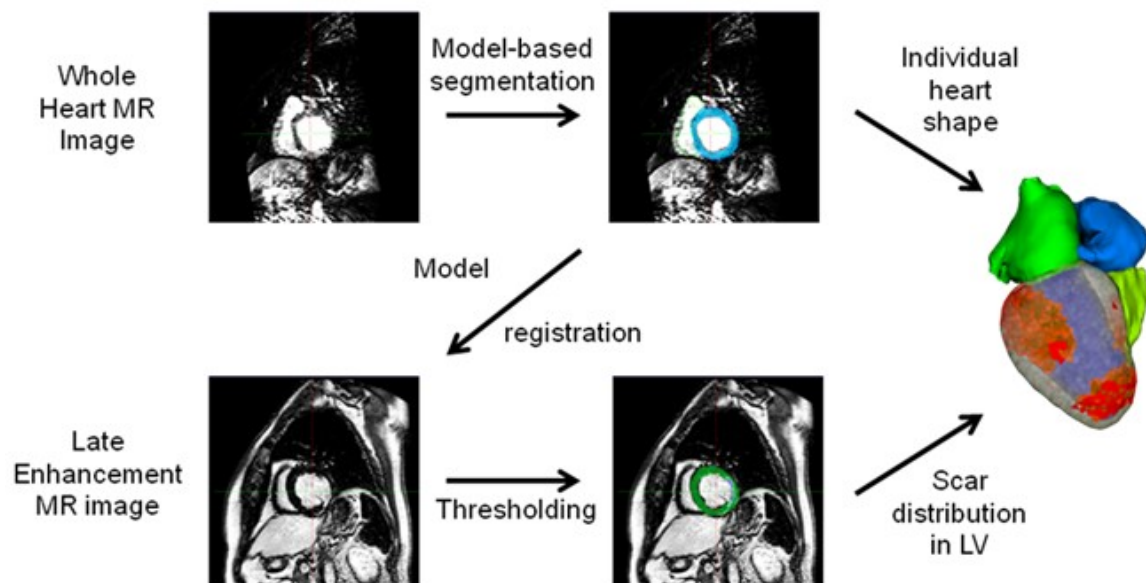


Figure 9 Diagram illustrating the processing steps for generating personalized heart models including the scar distribution in the left ventricle.

5.2. Vessel segmentation

The work on vessel segmentation builds upon a geometrical moment-based tracking algorithm that was initially designed for the lower limb vessel extraction and coronary arteries segmentation in CT angiography images. Its principle assumes that a vessel can be locally approximated by a cylinder. Then, analytical expressions of 3D geometrical moments of up to order two are used in association with local intensity information to compute the local orientation of the cylinder axis and its diameter. This algorithm has been revised to make it more robust for weak contrast and noisy data sets by regularizing the tracking direction, by construction a set of paths based on a multiple hypothesis testing procedure and by a graph-based method for selecting the optimal path. The method has, for instance, been used to complement cardiac models with the coronary vein tree that is relevant for the placement of the pacing lead in CRT treatment.

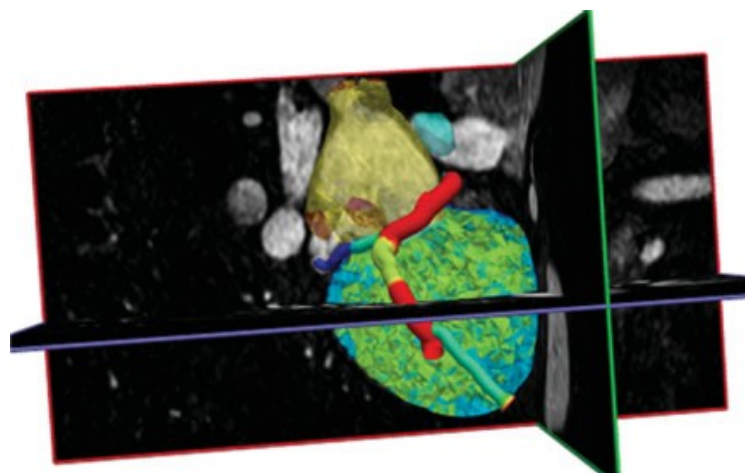


Figure 10 Model of the four chambers and the coronary venous tree derived from a three-dimensional whole-heart MRI data set.

5.3. Motion estimation

The quantification of cardiac motion and strain from image time series provides insight into how a pathology affects cardiac function in general and local motion and contraction of the LV myocardium in particular. For instance, the relative timing of regional myocardial tissue motion helps to identify the type of dyssynchrony of CRT candidates. For estimating motion, we developed the Temporal Diffeomorphic Free Form Deformation (TDFFD) algorithm (De Craene, M., et al., *Med Image Anal*, 2012. 16(2): 427-450) that represents the 4D velocity field by a B-Spline representation continuous in space and time. The motion field can be used to map a point in a reference frame to other image frames (Figure 11). The parameters of this deformation field are determined by registering the images of the time series to a selected reference frame. Within this registration process, volume changes of the myocardial tissue are penalized. The algorithm was initially developed and tested for 3D ultrasound images, where modality-specific artifacts make motion and deformation estimation challenging. Later on the algorithm was also adapted to tagged MR images to account for the degradation of the tagging pattern over time.

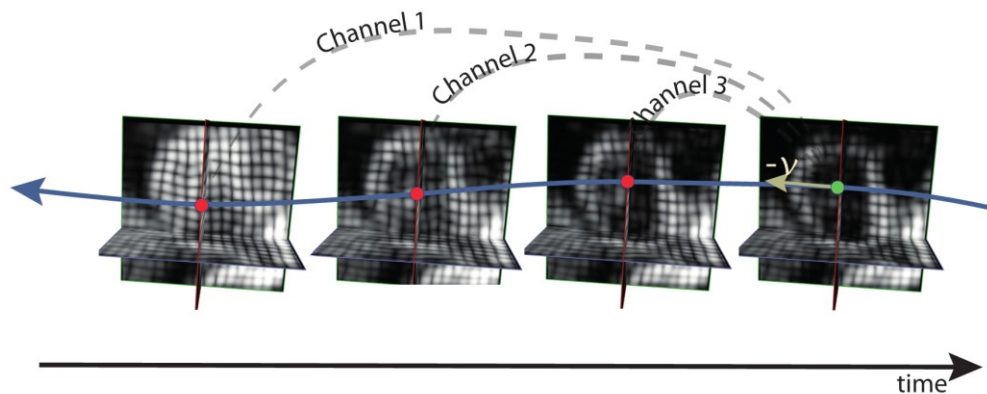


Figure 11 Point in a reference frame (green) that is mapped via the 4D motion field to other image frames (channels).

5.4. Aorta segmentation with pressure constraint

Biophysical and physiological properties manifest themselves in the temporal behavior of organs or anatomical structures. In particular, diameter changes of the aorta during the heart beat relate to vessel wall properties and pressure. For an idealized cylindrical vessel with linear wall material, the pressure as a function of distance along the vessel and time obeys the 1D wave equation. The pressure difference with respect to a reference point is proportional to the associated fractional radius change (FRC) with a proportionality factor related to Young's modulus describing tissue stiffness or to the pressure wave velocity. The idea of aorta segmentation with pressure constraint is to exploit this equation for stabilizing image analysis and measuring properties of the aortic wall.

To estimate diameter changes from a 3D CT or MRI image time sequence, a mean or reference image is derived and each image of the sequence is mapped to the reference image. The reference image is segmented to generate a binary image and this segment is then mapped back to each individual image. A

further mapping maps the reference segment to a cylinder, and is also applied to each of the segments in the sequence. The mappings can be used to determine the fractional radius change (FRC) between an image slice of the reference segment and an image slice of another segment at a distinct time point (Figure 12). The computed values are, however, corrupted by noise. Regularization is therefore applied with a constraint derived from the wave equation to ensure that the resulting FRC values satisfy both the data and the constraint. As the vessel wall properties change in reality along the aorta, the heart phase where the aortic flow is close to zero and the pressure along the aorta is uniform can be used to scale the FRC data to a surrogate of pressure. If a diastolic and systolic pressure measurement at some point along the aorta is available, the surrogate curve can be scaled to obtain absolute values of material properties (or wavespeed) along the aorta.

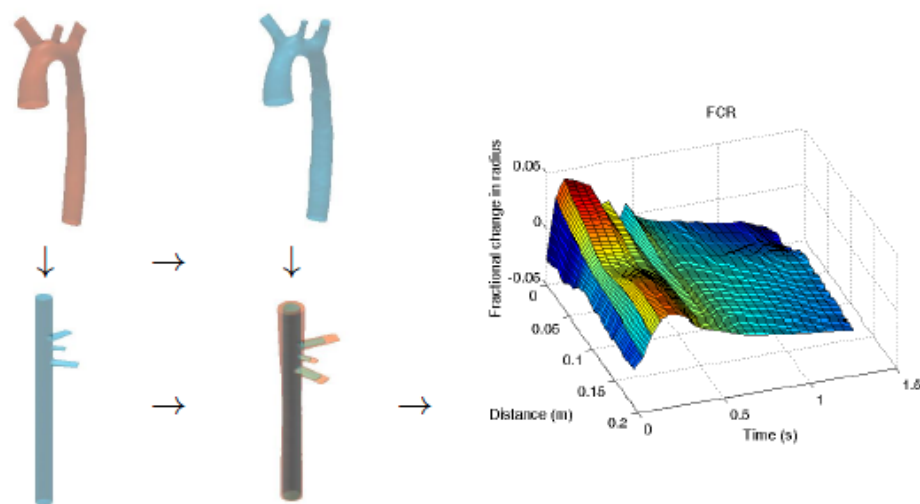


Figure 12 Diagram illustrating the computation of fractional radius changes along the aorta.

6. WP4 – Biophysical Model Personalization

Personalization of a biophysical model involves the specification of a set of patient-based physical and physiological parameters (e.g. the contractility of the muscle, the conductivity of the tissue...). The objective of this work package is to provide tools to personalize **generic** cardiac physiological models, i.e. to optimize their components so that their simulation matches closely the measurements in images and signals of a **specific** patient while based on meaningful biophysical models. This estimation task requires solving a usually large size inverse problem.

Model personalization is crucial to develop predictive models that can be used to plan the therapy of a given patient and to build decision support systems as developed in the application work packages WP5 - WP9. Given the complexity of this personalization, this work package coordinated and integrated the efforts of all partners in charge of model personalization. In particular, the Verdandi assimilation library was developed after a close analysis of the specific and generic aspects of the problems to be solved, and provided to relevant partners. Furthermore, several proof-of-concept studies have been performed.

6.1. Verdandi data assimilation library

After examining the needs of the application WPs in terms of parameter estimation, and collecting various specifications, the foundations of the data assimilation library – named Verdandi – have been built. The Verdandi library was designed with the utmost concern to ease interfacing with the partners' various simulation software. In this regard, the library architecture relies on three generic entities: a model, a data assimilation method and an observation manager. The library uses an interface for both the model and the observation manager entities. Once these interfaces have been implemented by the user, the various data assimilation methods provided by the library can be applied. In addition, Verdandi comes with a complete Python interface generated by Swig, which makes the various methods readily available in a command line environment.

The Verdandi library is distributed under the open source LGPL license, on a public dedicated web site (verdandi.gforge.inria.fr). It now contains about 60,000 lines of C++ code, compilable with ease on all major platforms. It contains all major data assimilation algorithms of both variational and sequential types, and in particular: optimal interpolation (also known as BLUE, for Best Linear Unbiased Estimator); space-time variational estimation (also known as 4D-Var, with an interface to the NLOPT optimization library); extended Kalman filtering and reduced-order version; unscented Kalman filtering (not requiring differentiated and adjoint forms of the simulation software) and reduced-order form. A complete documentation is provided, with

Verdandi generic library for data assimilation

INTRODUCTION	CONTENTS	DOCUMENTATION	DOWNLOAD
VERSION 0.8	VERSION 0.9	VERSION 1.0	VERSION 1.1
VERSION 1.2	VERSION 1.3		

Verdandi User's Guide

USER'S GUIDE

[Introduction](#)

[Getting Started](#)

[Dependencies](#)

[Assimilation Methods](#)

[Example Models](#)

[Observations](#)

[Tools](#)

[Plugging in Verdandi](#)

[Debugging](#)

[Python](#)

API REFERENCE

[Classes](#)

[Class List](#)

[Class Hierarchy](#)

[Class Members](#)

Functions

[Search for](#)

[Support](#)

Verdandi is a generic C++ library for data assimilation.

Verdandi is currently developed at [INRIA](#). It aims at providing methods and tools for data assimilation. It is designed to be relevant to a large class of problems involving high-dimensional numerical models.

To guarantee the highest performance, the library is implemented in C++. In addition, Verdandi provides a Python interface generated by [Swig](#).

Models implemented in Fortran, C, C++, Python, ... can be plugged to Verdandi using either a C++ or Python interface.

Verdandi is provided under the GNU Lesser General Public License (LGPL).

Scientific context

Data assimilation is the process of combining different sources of information in order to better estimate the state of a system. By extension, some parameters can also be estimated. These methods were originally introduced to deal with uncertainties present in models pertaining mostly to geophysics, but it is now widely recognized that they have a tremendous potential in many other applications (see euHeart example below).

Whether the system be biological, environmental, mechanical, etc., the main sources of information are always a numerical model, observations and error statistics. Data assimilation methods can be written independently of the system to which they are applied, and each method can be applied to a wide class of systems. Therefore methods are generic and can be put together in a library.

What is Verdandi for?

What is Verdandi designed for?

Figure 13 Snapshot of the Verdandi online User's Guide introduction (verdandi.gforge.inria.fr).

- A detailed User's Guide – both available online with web navigation (Figure 13) and search tool (see below figure), and as a pdf document in a book format – presenting the various data assimilation procedures available, and the details of the library usage (installation, interfacing with simulation software, configuration files, etc.).
- An API Reference section (online), defining the classes implemented in the library, generated from the software itself (and detailed comments therein) with the Doxygen documentation system, which ensures permanent compatibility with the software updates.

We also point out that – since the release of the original version – some extensive parallel features have been introduced in the library, with additional funding from the VPH-Share European project. Namely, the main data assimilation algorithms have been parallelized (using MPI), and the library can interact with parallel simulation software handling the simulation data in a distributed manner (PETSc standard).

6.2. Training and expertise transfer

Two training workshops have been organized during the project:

- One during the first year (14-15 October 2008, Paris) to present some methodological guidelines regarding parameter and state estimation in biophysical models, and to gather and discuss the participants' needs.
- The second right after the release of the Verdandi library, (30 June - 1 July 2011, Paris) to present the specifics of the software library (first day) and interactively discuss integration aspects with the partners (second day).

In addition to the library documentation itself that is directly available in the distribution, a technical report was produced to present a survey of the major

principles of data assimilation procedures, together with detailed examples of applications in cardiac modeling. The examples

- estimation of passive law parameters in cardiac mechanical model (WP5) and
- estimation of solid constitutive parameters in FSI arterial model (WP9)

were chosen and presented in coordination with the application WPs.

During the library development, the WP4 developers have worked in close collaborations with various application WPs – in particular with WP7 and WP9 – in order to validate the strategy on how to integrate the assimilation library in the various codes, mostly based on the implementation of software prototypes. In this process, expertise has also been provided to formulate and solve specific personalization problems arising in these WPs. After the software release, WP4 has provided assistance on the use of the software, in particular as regards interfacing with simulation software, and in several instances on the choice of well-suited data assimilation methods, e.g. in

- WP5 for integration of Verdandi with the Sofa code in order to estimate mechanical parameters.
- WP6 to formulate a data assimilation strategy pertaining to the estimation of electrophysiology model parameters based on depolarization isochrones, and to interface the Verdandi library with the Sofa code accordingly.

6.3. Proofs of concept studies

While developing the Verdandi data assimilation library, we have also performed proofs-of-concept studies to assess and demonstrate the use of data assimilation concepts and algorithms in cardiovascular modeling applications:

- **Estimation of stiffness parameters in blood vessel walls.** In collaboration with WP9, we considered the blood flow in an idealized aneurysm (see Figure 14), modeled with full fluid-structure interaction, and the problem of estimating the stiffness in the vessel wall. The geometry is divided into 5 regions and the stiffness is lower in the region close to the aneurysm. We then launch the personalization procedure based on the reduced-order Unscented Kalman Filter (RO-UKF), using synthetic data – namely, generated by a reference simulation of the model – of the wall displacements. Starting the estimation with a homogeneous nominal value of Young's modulus, we retrieved the expected parameter values (Figure 14 and Bertoglio, C. et al., Int J Num Meth Biom Eng, 2012. 28(4): 434-455).

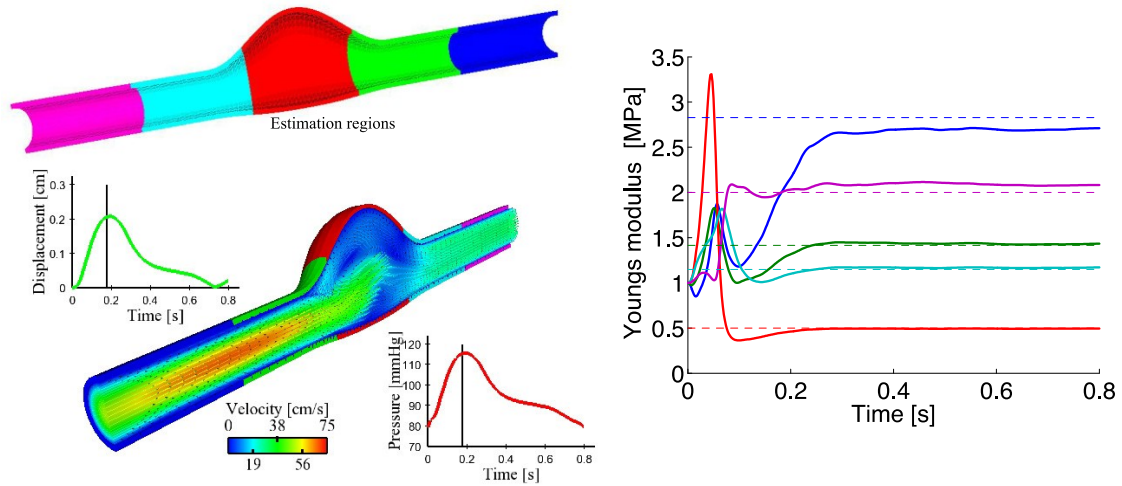


Figure 14 Estimation of stiffness parameters in idealized aneurysm: parameter regions (top left); fluid-structure simulations (bottom left); estimated parameter values in regions (right; reference in dashed lines).

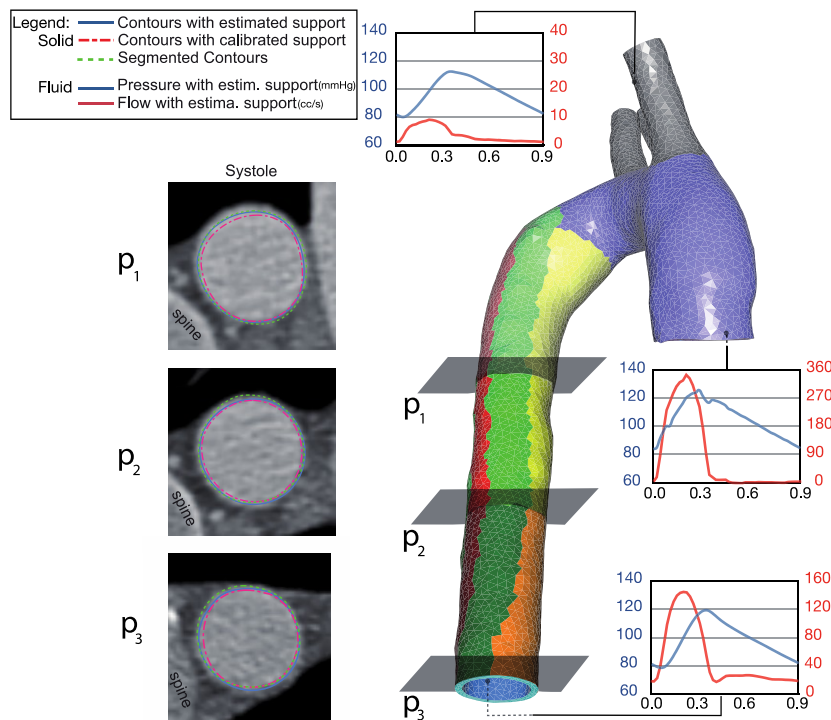


Figure 15 Patient-specific aorta model with estimation of boundary support parameters based on image data; comparison of personalized model with segmented wall in 3 CT cross-sections (left); parameter regions (right).

- Estimation of boundary condition parameters for aorta with real data.** In collaboration with the Reo Inria team and the CardioVascular Biomechanics Research Lab of Stanford University, we addressed the problem of personalizing arterial models (aorta) with actual image data, using specific parameterized boundary conditions to model the effect of surrounding structures. We considered full fluid-structure coupling in the model, with large displacements and strains in the wall modeling, as is essential for the aorta. Localized boundary condition parameters were

estimated using the RO-UKF approach. The resulting personalized model was assessed by comparing the deforming walls with segmented dynamic image data (Figure 15 and Moireau, P., et al., Biomech Model Mechan, 2012. published online.).

- **Estimation of contractility parameters in infarcted heart.** In collaboration with the Henri Mondor Hospital, we demonstrated the use of an effective combination of data assimilation algorithms (including RO-UKF) to estimate regional contractility parameters in a beating heart model using actual clinical data – notably cine-MRI – for an infarcted heart. Such parameters are most meaningful to characterize the location and seriousness of the infarct. In turn, the automatic personalization of these parameters dramatically enhances the model predictivity (Figure 16).

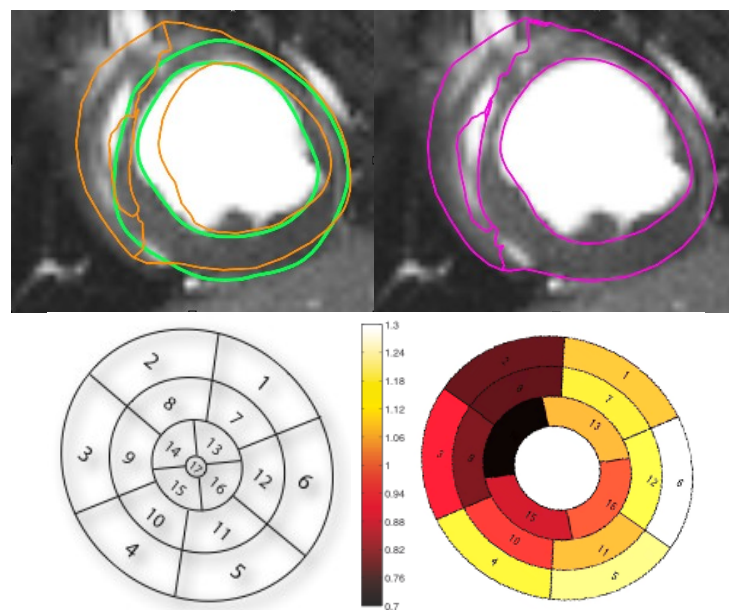


Figure 16 Contractility parameters estimation in infarcted heart; end-systolic MR compared with left ventricle segmentation (green), model prior to (orange) and after (purple) personalization (top); bull's eye view of AHA regions and estimated contractility parameters (bottom; high values i.e. light colors correspond to healthy tissue).

7. WP5 – Cardiac Resynchronization Therapy

The increasing prevalence of congestive heart failure (CHF) is mainly caused by the steadily increasing number of heart attack survivors. In total, there are about 10 million patients treated for heart failure in the EU, corresponding to about 4% of the adult population, and resulting in 2% of the total health care costs. In a large subgroup, CHF is associated with abnormal electrical activation of the left ventricle. In these patients, Cardiac Resynchronisation Therapy (CRT) has recently been shown to be an effective treatment. However, since about one third of the patients do not respond to this very expensive (>€20.000) therapy and might even worsen their symptoms, significant controversy remains regarding optimal patient selection. Additionally, there might be a number of potentially successful responders who are currently not considered for the therapy. The ability to predict an individual response to CRT, thus reducing the unsuccessful response rate, and identifying the best methods of delivering this treatment (e.g. lead positioning, pacemaker setting), will have a real impact on CHF treatment.

The goal of application package WP5 was the development of methods for improved CRT patient selection and in-silico CRT therapy planning. This application package uses image processing techniques and computational models jointly with algorithms to personalize multi-scale electro-mechanical models of the heart. In particular, a CRT planning environment has been set up and new quantitative indices for patient selection have been developed. Finally, a simulation environment to optimize the patient specific therapy response with respect to the lead positions and pacing device settings has been developed and validated.

7.1. CRT Planning environment

A CRT planning environment has been set up (Figure 17) that brings together tools and results from multiple teams and other workpackages like WP3. The workflow oriented GIMIAS environment which has been designed for the development of biomedical imaging prototypes, was used as a basis for integration and many tools - mainly the ones related to the anatomical building – are implemented as GIMIAS plug-ins.

The first step towards a personalized CRT simulation is the extraction of the anatomy. We have developed a semi-automatic segmentation technique based on atlases with population data that can be applied to whole-heart CT or MR images. In addition, the user has manual correction tools if the segmentation is not accurate enough. Functional information such as tissue viability, which is crucial for interventional planning, can also be extracted from late enhancement MRI (see Figure 9). Finally, the coronary vein tree is extracted using vascular segmentation techniques (see Figure 10) since it will constrain the lead placement.

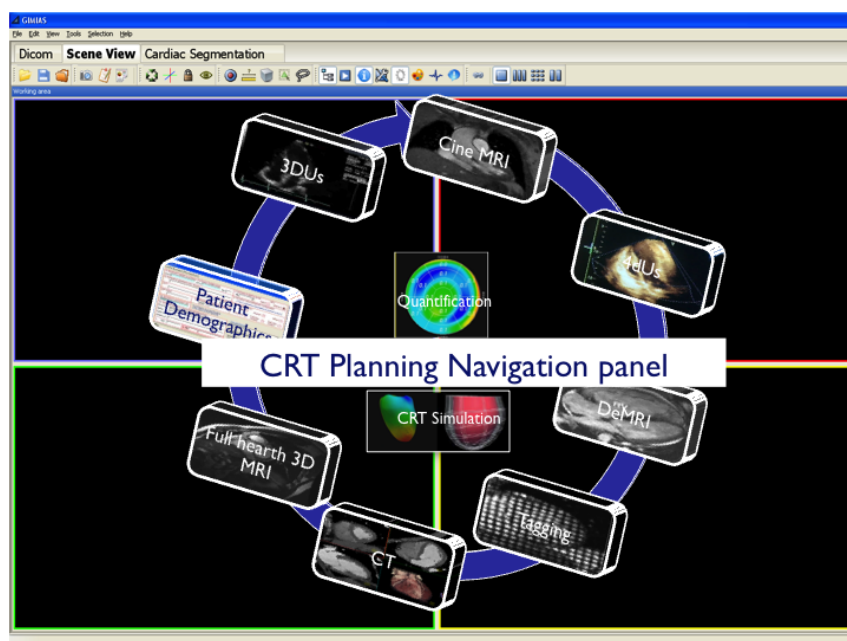


Figure 17 CRT planning navigation panel, where the user can choose which processing of the medical data wants to do or to visualize.

After the anatomical personalization, mechanical and electrophysiological cellular models, most of them available in the [CellML repository](#), are coupled to monodomain activation and finite deformation mechanics within continuum-based simulation codes optimized for high performance parallel implementation. The key step is the personalization of conductivity and stiffness parameters as well as identifying appropriate boundary conditions, since these variables cannot be measured in vivo and are very critical for having more realistic electromechanical simulations. Most of these codes have been implemented in Open Source platforms such as [OpenCMISS](#) and [Chaste](#), making collaboration between different research groups easier.

Once electromechanical simulations are obtained, they are post-processed and compared with information and other indices extracted from imaging and signal data, such as deformation fields from echo images, contact mapping data or pressure information.

7.2. New indices for patient selection

It has been proven that a typical abnormal motion in the septum (the wall that separates the left and the right ventricle) called septal flash can lead to better response to CRT therapy. Septal flash consists of a very fast inward-outward motion of the septum. In order to detect and quantify septal flash, we have created a motion atlas of normal patients from 2D Ultrasound and compared new pathological patients to the normality atlas, drawing abnormality maps (Figure 18). The abnormality maps show in blue abnormal inward motion, in red abnormal outward motion and in white normal motion. The axes of the graphic are time in the x axis and the position in the septum in the y axis. Septal flash, in these abnormality maps, is clearly shown by a vertical blue stripe followed by a vertical red stripe. A study has been performed where datasets of 88 patients

were analyzed (Duchateau, N., *Ultrasound Med Biol*, 2012. 38(12):2186-2197). CRT responders showed significantly higher reduction of abnormalities. Non-responders conserved abnormal septal motion at the end of the isovolumic contraction (IVC). A specific inward-outward motion of the septum during IVC predominated in responders and was corrected at follow-up.

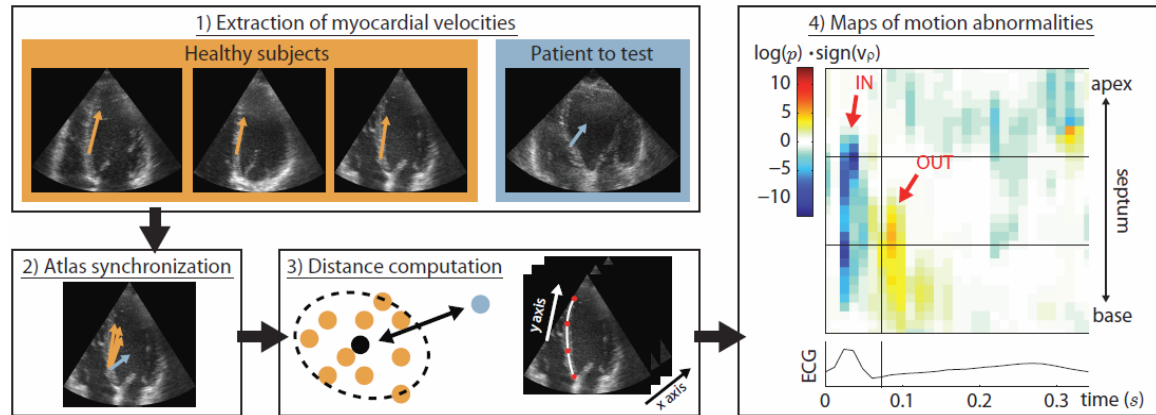


Figure 18 Block scheme of the motion anomaly quantification based on an atlas of a population of normal patients.

7.3. Simulation-based prediction of CRT treatment response

To predict the acute response to CRT, an electromechanical model of the left and right ventricular myocardium was personalized (Sermesant, M., et al., *Med Imag*, 2012. 16(1): 201-215). The patient-specific anatomy was derived from anatomical MR scans and the heart motion from cine MR sequences. Invasive measurements from endocardial mapping and a pressure catheter were used to personalize electrophysiological parameters such as the tissue conductivity and mechanical parameters such as the contractility. The acute effects of pacing on pressure development were predicted with the in silico model for several pacing locations on two patients, achieving good agreement with invasive hemodynamic measurements reference measurements (see Figure 19 for the results for one patient). The results demonstrate the potential of physiological models personalized from images and electrophysiology signals to improve patient selection and plan CRT, but validation on a larger patient population is needed in the future.

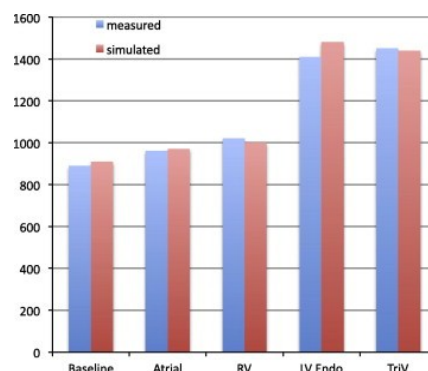


Figure 19 Simulated and measured (dP/dt) max for different pacing locations of a patient.

8. WP6 – Cardiac Radiofrequency Ablation

A major component of the increasing rate of cardiovascular diseases is the rise in cardiac arrhythmias caused by structural disorders of the heart such as myocardial scarring following myocardial infarction that in turn produces life threatening arrhythmias such as ventricular tachycardia (VT). Additionally, the prevalence of atrial fibrillation (AF), which is more and more recognized as having a major impact on the patient's quality of life and prognosis, is related to age and roughly doubles with each advancing decade, from 0.5% at age 50–59 years to almost 9% at age 80–90 years. The clinical understanding and treatment of these patients is complicated and includes a wide range of therapies, going from pharmaceutical to devices (pacemakers and ICDs) and interventions (surgical or radiofrequency ablation).

In a subgroup of AF patients, the use of radiofrequency ablation (RFA) has shown to be an effective cure. However, in many cases, the procedure has to be repeated a number of times with some patients receiving little long-term benefit. With well over 4.5 million patients with AF in Europe, RFA is having a major impact on rising healthcare costs. VT is now commonly being treated with the insertion of intra-cardiac defibrillators; however RFA has the potential of being a better and cheaper alternative therapy. Improving the clinical understanding of the structural and mechanistic determinants of arrhythmias and incorporating this in optimizing patient selection, procedure planning and guidance for RFA promises increased success rates of the procedure.

Within this workpackage, electrophysiological and elastomechanical models of the heart have been developed for cardiac arrhythmias such as AF and VT. Particular attention was paid to approaches that personalize and optimize the models using patient specific data. Results include methods to generate the patient-specific atrial anatomy including multi-layer muscle fiber orientation and an approach to personalize the left ventricular electrophysiological parameters. The methods have, for instance, been used to predict the outcome of RFA redo procedures for AF and to support RFA procedures for VT by predicting VT re-entry patterns. In addition, ECG imaging has been improved and first results have demonstrated that re-entry cycles and related exit points in VT can be reconstructed with ECG imaging.

8.1. Atrial fiber architecture

The electrical excitation of the human atria is determined by the muscular structure of the atrial wall. Up-to-date imaging technology is only able to image the inner surface of the atria. Electrophysiological simulations on models derived from such data can only provide a rough estimate of the real excitation sequence of the atria. A method to introduce complete, multi-layer muscle fiber orientation in patient-specific atrial anatomy models has been developed (see Figure 20 for an example). The augmented anatomy models allow for a realistic simulation of sinus rhythm and also fulfill the necessary prerequisites to simulate atrial arrhythmias. In addition, the enhanced anatomical models were coupled with a newly developed model of the regional atrial electrophysiology. This approach may provide more reliable insights into the mechanisms leading

to AF, for instance by investigating the spontaneous initiation of atrial fibrillation through ectopic activity in the pulmonary veins.

Models with incorporated atrial fiber orientation have been made available to various research groups (Oxford, Auckland, Graz, Baltimore). Additionally, one patient-specific atrial model with fiber orientation is publicly available through the anatomical model database AMDB.

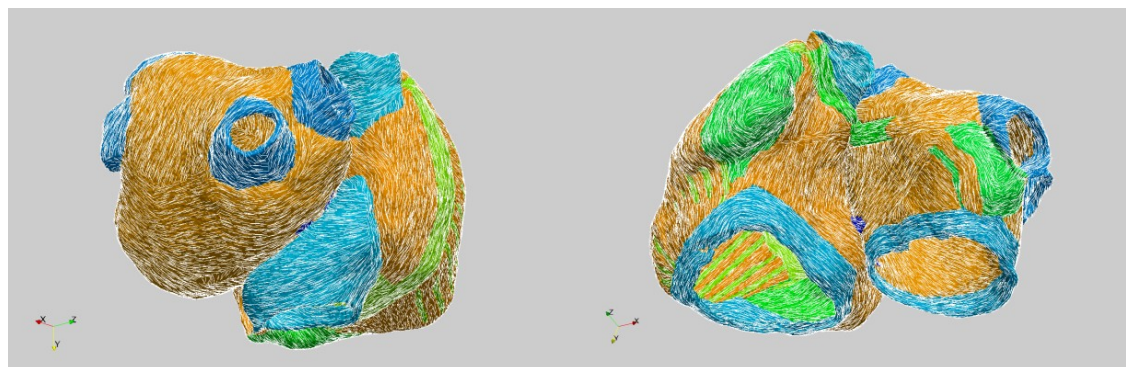


Figure 20 Anatomical model of an AF patient's atria. Colors indicate different myocardial regions and white lines show the local muscle fiber orientation.

8.2. Prediction of outcome of RFA redo procedures

Radio-frequency ablation therapy is a minimal invasive treatment against AF. Although being a curative treatment, many persistent AF patients need to undergo several ablation procedures until being cured from the disease. Computational models of the atria bear the potential to evaluate the outcome of ablation procedures and to guide redo-procedures. For this purpose, a pipeline to transfer ablation scars identified in late Gadolinium enhancement MR images into patient-specific atrial anatomy models has been developed. Using fast Eikonal simulation approaches, a sensitivity analysis can reveal incomplete ablation of lesions. It can thereby help to predict AF recurrence, visualize breakthrough pathways and guide redo-procedures. The tool may in particular support clinicians by providing clearer 3D visualization of the cause for AF recurrence and by virtually testing possible ablation countermeasures (Figure 21). The approach has been tested on 5 patient datasets and can also include information of regional fibrosis in the patient's atrial anatomy models based on late enhancement MRI data.

8.3. Personalization of EP models from ventricular endocardial mapping

By combining MR imaging, intracardiac non-contact mappings and biophysical modeling, we have achieved the full personalization of electrophysiological models of the right and left ventricles on 8 patient datasets. Personalization of biophysical models is a novel but essential task in order to build predictive models than can help physicians to plan therapies.

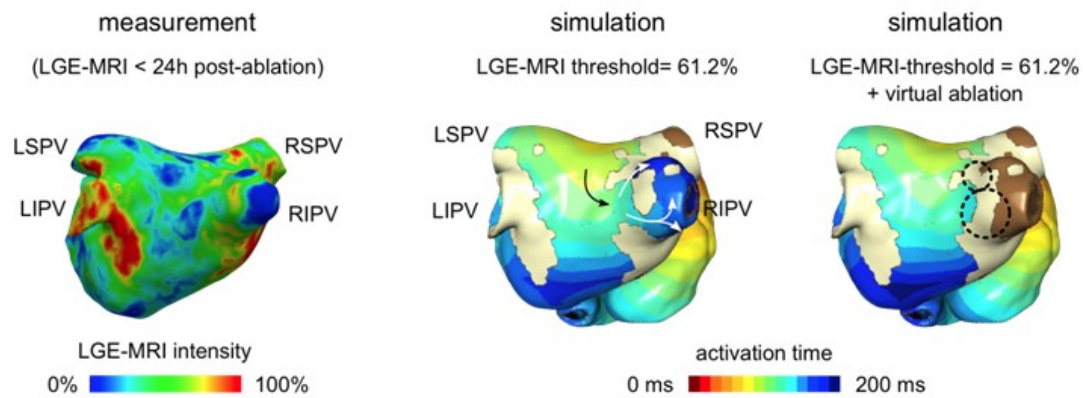


Figure 21 Late Gadolinium enhancement (LGE) MRI intensity on a 3D shell of the left atrium and corresponding patient-specific atrial models with scar locations derived (left). A virtual ablation was performed to close an identified incomplete radio-frequency ablation lesion (right).

Three types of patient-specific information have been used for the personalization: anatomical, pathological and functional data. A pipeline of tools has been developed to create personalized meshes of the two ventricles eventually including regions of scar and peri-infarct zones from anatomical and late enhancement MR images of the cardiac cavities. Furthermore, by registering activation times and action potential duration maps measured from intracardiac non-contact mapping on the patient-specific mesh of the two ventricles, the parameters of the Mitchell-Schaeffer (MS) model were optimized such that the simulated depolarization and repolarization times matches the observed ones (Relan J., et al., J R Soc Interface Focus, 2011. 1(3):396-407). Note that due to the limited amount of information that can be observed from those electrophysiology endocardial maps, we chose to model patient specific ventricular electrophysiology based on the phenomenological MS model for its compact and simple description of restitution properties.

As a result of this personalization step, maps of parameters that capture structural and functional heterogeneities of the myocardial cells can be computed. One of such parameter that can be mapped is the electrical diffusivity coefficient which partially controls the conduction velocity of the depolarization wave and whose value is largely affected by the presence of scar tissue. Another important parameter is a parameter controlling the slope of the action potential duration restitution curve and therefore which characterizes the local refractoriness of the tissue. This personalization steps leads to a predictive model of the ventricular electrophysiology. Its predictive power can be evaluated for instance by applying a given stimulation protocol and then measuring the discrepancy between simulated isochrones and measured ones (Figure 22).

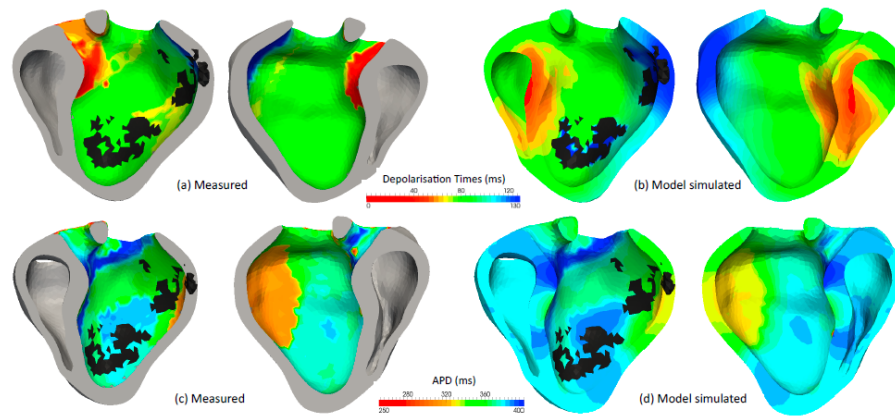


Figure 22 Comparison between the measured (left) and simulated (right) Depolarization Time isochrones (upper row) and Action Potential Duration (lower row). Note that the DT and APD are only measured on the LV surface whereas they are simulated on the whole heart.

8.4. Prediction of VT re-entry patterns

For the study on Ventricular Tachycardia (VT), we have focused on cases of ischemic VT where the main cause of re-entry is related to the presence of viable tissue surrounded by scar tissue. In this context, a framework to test *in-silico* the inducibility of VT has been developed by evaluating under which condition it is possible to create a re-entry pattern. This aims at reproducing the VT stimulation study, as known as VT-Stim, which is often performed prior to an implantation of defibrillators or VT radio-frequency ablation. The proposed approach consists in applying a set of stimulation protocols at various locations in the right and left ventricles of a personalized electrophysiological model of the heart and then automatically detecting the occurrence of monomorphic VT, the ventricular regions causing those arrhythmias and corresponding to exit points, the location and nature of the re-entry patterns and finally the regions from where VT can be induced. An important advantage of this approach is the possible to test the inducibility of VT from many more stimulation sites than can be done during a real VT-Stim procedure during which the heart is mainly stimulated around the apex of the right ventricle. Furthermore, an important outcome of the computational VT-Stim is the ability to locate exit points which are possible candidate regions for a radiofrequency ablation procedure.

The proposed approach has been evaluated successfully on 2 patients for whom a non-contact electrophysiological mapping system was used during a real VT Stim procedure. In those 2 cases, VT could be induced during the procedure but also *in-silico* by performing a similar stimulation protocol on personalized electrophysiological models of the right and left ventricles. Furthermore, similar re-entry patterns could be observed (Figure 23) and the location of exit points has been shown to match regions of high heterogeneity in terms of action potential duration (APD) restitution slope parameters.

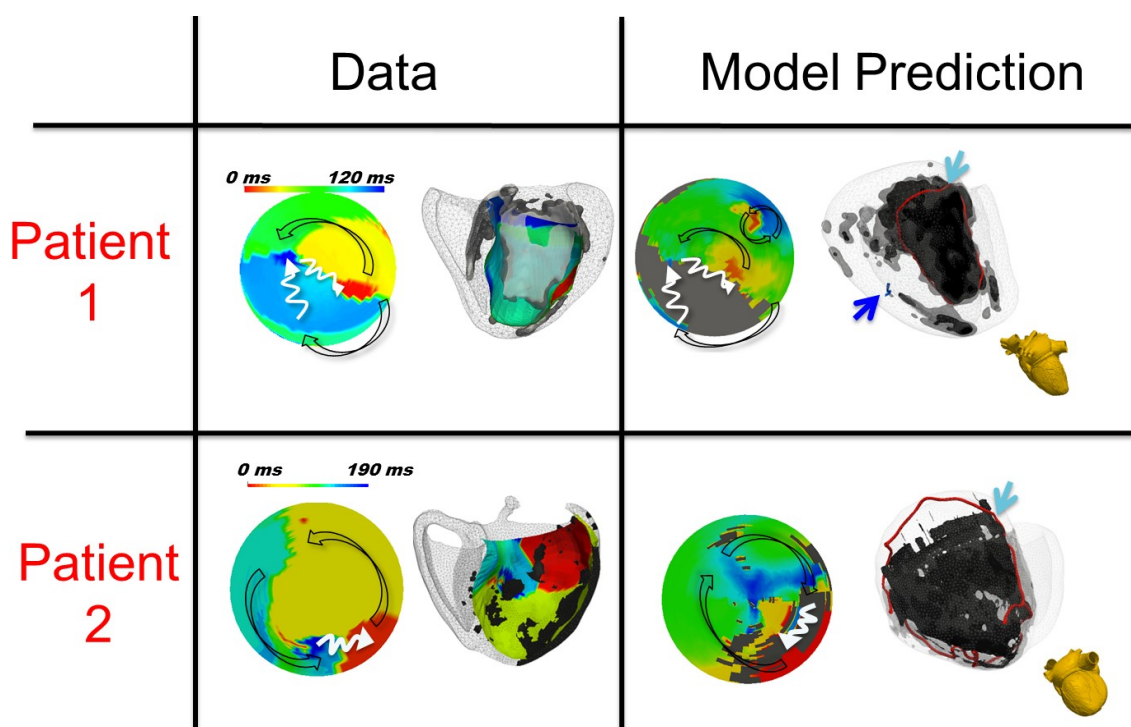


Figure 23 Comparison between the predicted VT isochrones (right) as a bull's eyes plot and the measured ones (left) for two patients that undergone a VT Stim procedure; the 2 circular arrows on the plots show the re-entry circuits while the red region corresponds to the location of exit points; the estimated re-entry circuit (red curve) is displayed on the right, the scar regions being shown as black regions.

8.5. ECGI during VT Stim

ECG imaging (ECGI) is a technique for the reconstruction of cardiac electrophysiological signals from ECG measurements. To establish the three-dimensional source distributions in the heart that have caused the measured ECG, a precise patient-specific model of both the heart and thorax is needed, and a strongly ill-posed inverse problem has to be solved mathematically.

Comprehensive sources of clinical data have been merged to generate the required models: different MRI data sets haven been co-registered and segmented into multiple organs and a whole heart model, including scar tissue from gadolinium delayed enhancement MRI. Body surface potential maps were recorded both pre-operatively and in the catheterization laboratory. To localize the related electrodes on the thorax in a clinical environment, a new method was developed using X-ray angiography images. Along with the body surface potentials, concurrent EnSite intracardiac potential and activation time measurements were acquired that serve as a ground truth for a validation of the ECGI method. For the VT datasets, first results have demonstrated that re-entry cycles and related exit points can be reconstructed with ECGI. The unique nature of this work is in the quality of the comprehensive models and the closed workflow using completely non-invasive data acquisitions, along with the otherwise rare ground truth data collected in the left ventricle. The non-invasive reconstruction of cardiac electrophysiology in combination with anatomical information from MRI may be used in future to diagnose and monitor cardiac arrhythmias before interventions, and it may both shorten the duration and increase the success of interventions for radio-frequency ablation therapy.

9. WP7: Heart Failure

WP7 focuses on heart failure (HF) in two important settings. The first focus is the use of left ventricular assist device in patients with acute or chronic severe HF. HF is rapidly becoming an epidemic, a fact confounded by the severe lack of donor hearts as transplant is currently the only established long term solution. To create a bridge to transplant, left ventricular assist devices (LVADs) are often surgically implanted. In a recent and highly promising development, a small but significant subpopulation (5%) with implanted LVADs recover, undergoing reverse cardiac remodeling to the point where the LVAD can be removed without the need for transplantation. Thus the potential to optimize LVAD function and surgical interventions is significant.

The second focus is on patients with complex congenital heart disease where the morphological right ventricular acts as the main pump maintaining the systemic circulation. The great success of palliative surgery in infancy and childhood for these patients means that there are now large numbers reaching adolescence and adulthood. Unfortunately the systemic right ventricle in most of these patients appears unable to continue to maintain good pump function and starts to fail. For some of these patients there is a high risk way forward of retraining the systemic left ventricle which has lost most of its mass due to pumping against the low pressure pulmonary circulation. Following retraining (pulmonary artery band) an arterial switch can be performed in conjunction with switching of the venous flow in the atria so that the morphological left ventricle becomes the systemic pumping chamber. Although this will confer much better long-term outlook, the procedure is very high risk with up to 50% mortality. Optimized patient selection and timing of this intervention has a major impact on the morbidity and mortality of this important group of patients.

Within this work package strongly coupled, multi-scale fluid-solid mechanical models of the heart were used to develop a framework with the potential to direct interventions that treat the remodeling of myocardial tissue. The resultant multi-scale whole organ models have enabled the visualization of novel clinical performance indices including the spatial-temporal distributions of stress, work, and energy consumption that cannot be currently directly imaged. The model has been specifically customized for device design and tuning for Berlin Heart Left Ventricular Assist Device (LVAD) recipients and for surgical treatment of congenital patients. From the customized models we have developed and validated, there is now a predictive tool for optimizing these interventions available at KCL based on the performance indices, the fluid velocity fields within the cardiac chambers and the mechanisms underlying remodeling in Heart Failure.

9.1. Fluid-Structure models for simulating LVAD cardiac function

Numerical simulations provide a unique approach for investigating the impact of left ventricular assist devices (LVADs) on the pump function of the heart. To this end, the fictitious domain (FD) method was incorporated within a non-conforming coupled fluid–solid mechanics solver creating a model capable of

capturing the full range of cardiac motion under LVAD support, including contact of the cannula with the ventricular wall. To demonstrate and verify the properties of the applied method, convergence studies were performed showing linear convergence for both a fluid only problem with an immersed rigid body, as well as a fluid–solid coupled problem with a fluid immersed rigid body interacting with the coupled elastic solid. The model was implemented on a left ventricular (LV) geometry constructed from human MRI data. Simulations were performed to compare LV function with an FD prescribed LVAD cannula and with a cannula applied as a Dirichlet boundary. Good agreement was observed between the simulations for myocardial deformation, major flow features and rates of energy transfer.

Furthermore, an LV simulation was performed to bring the ventricular wall into contact with the cannula, demonstrating the applicability of the model to investigating LV function under LVAD support. In this work we have integrated novel modifications of the standard Newton–Raphson/line search algorithm and optimization of the interpolation scheme at the fluid–solid boundary to enable the simulation of fluid–solid interaction within the cardiac left ventricle under the support of an LVAD. The line search modification produced close to an order of magnitude improvement in computational time across both test and whole heart simulations. Optimization of element interpolation schemes on the fluid–solid boundary highlights the impact this choice can have on problem stability and demonstrates that, in contrast to linear fluid elements, higher order interpolation produces improved error reduction per degree of freedom. Incorporating these modifications enabled modeling of a full heart cycle under LVAD support. Results from these simulations show that there is slower clearance of blood entering the chamber during early compared to late diastole under conditions of constant LVAD flow.

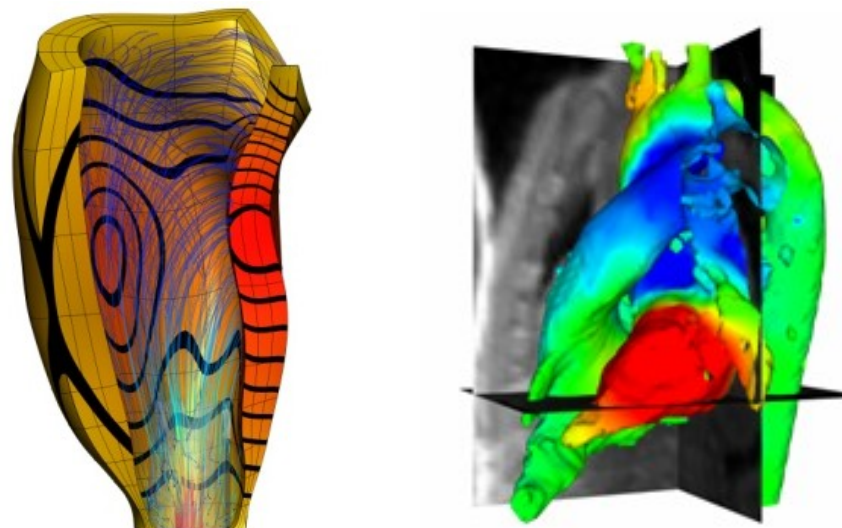


Figure 24 Coupled fluid mechanical simulation (left) of the interaction between a ventricular assist pump and cardiac contraction (stream lines show velocity and contours show pressure) and non-invasive estimation of pressure in the heart from comprehensive MRI data (right).

9.2. Optimal LVAD flow regimes for promoting cardiac remodeling

Applying the coupled fluid-solid mechanics cardiac LVAD framework to a patient customized geometry, we have provided the first numerical investigation into the impact of aortic valve opening and LVAD flow synchrony on ventricular hemodynamics and myocardial mechanics. Specifically, the developed model has been applied to investigate the mixing of blood within the left ventricular chamber, as well as the efficiency of myocardial work transduction under different LVAD flow protocols. From these results we have enabled a unique analysis of the impact of LVAD flow on ventricular unloading and the pooling of blood in the ventricular chamber. Six simulations were performed covering a range of LVAD flow protocols (constant flow, sinusoidal in-sync and sinusoidal counter-sync with respect to the cardiac cycle) at two different LVAD flow rates chosen so that the aortic valve would either open (60mL/s) or remain shut (80mL/s). From these simulation results, the opening of the aortic valve resulted in the spatial homogenization of myocardial work across the left ventricle. When the valve remained shut, this effect was partly replicated by increasing LVAD out-flow during the contractile phases of the cardiac cycle. Regardless of valve opening, increasing LVAD flow during myocardial contraction and decreasing it during diastole improved the mixing of blood in the left ventricular cavity. These results show that varying LVAD flow in-sync with the cardiac cycle improves both myocardial unloading and the residence times of blood in the left ventricular cavity.

9.3. Anatomy and diastolic filling in systemic right ventricular patients

Pediatric patients with hypoplastic left heart syndrome (HLHS) rely solely on the right ventricle, resulting in anatomic maladaptations that can significantly compromise diastolic efficiency and lead to heart failure. Clinical indices to evaluate diastole are generally derived from the adult left ventricle, limiting their relevance to patients with HLHS. Using personalized blood flow simulations, we have shown the effect of the ventricular cavity shape and tricuspid inflow typology on the filling dynamics to provide new directions for assessing diastolic function in these patients.

Magnetic resonance imaging data were used to generate personalized models of 8 patients with different prognoses after stage I of the Norwood procedures. Two of these patients were also modeled after stage II. Numeric simulations were performed to analyze the interaction between blood flow and the myocardium during diastole. The filling dynamics were characterized by the formation of an organized structure of swirling blood (vortex ring). This was strongly influenced by the ventricular shape and the timing. Biphasic rather than fused inflows and more elliptical than spherical cavities were found to increase the intraventricular pressure gradients and the filling capacity by optimizing the energy transfer between blood flow and the myocardium. This resulted in a better flow propagation and higher tissue velocities and displacements.

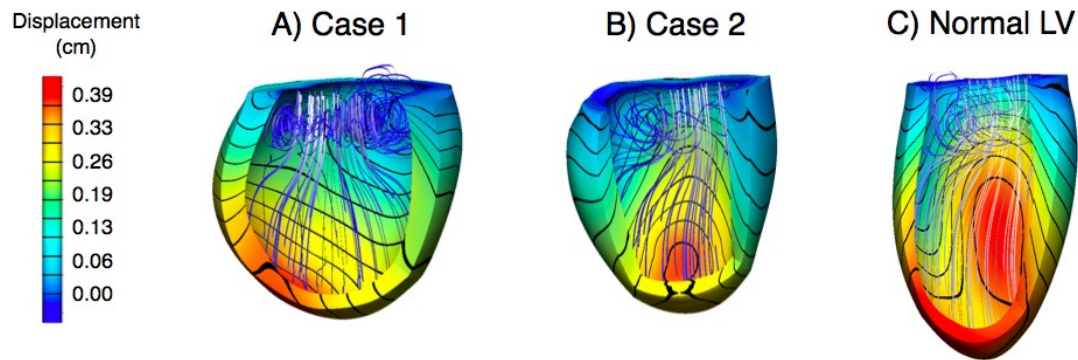


Figure 25 Instantaneous streamlines of blood flow and iso-contours of myocardial displacement at the peak E-wave of diastole in two baseline HLHS patients (A-B) and a normal left ventricle (C).

9.4. Novel metric for characterizing systemic right ventricular patients

Fluid-structure interaction simulations have been performed to analyze the diastolic function in hypoplastic left heart patients, who underwent the first stage of a three-step surgical palliation and whose condition must be accurately evaluated to plan further intervention. The kinetic energy changes generated by the blood propagation were found to reflect the intraventricular pressure gradients, giving indications on the filling efficiency. This suggests good agreement between the 3D model and the Euler equation, which provides a simplified relationship between pressure and kinetic energy and could therefore be applied in the clinical context. Applying these results we have shown that the variations in the kinetic energy associated with the blood motion reflected the base-to-apex pressure difference and the efficiency of filling, to provide a new metric to assess diastolic function in these patients.

10. WP8 – Coronary Artery Disease

Coronary artery disease (CAD) is the major cause of mortality worldwide and causes a high economical burden. For example, the cost associated with CAD across the EU corresponds to almost 1% of 1999 GDP and to almost 11% of total national health expenditure in the UK. Developing improved modalities for the non-invasive and invasive diagnosis and treatment of coronary disease is, therefore, an economic necessity and important for increased quality of life.

A stenosis in a coronary limits the blood supply to myocardium. Presently, the most frequently applied revascularization therapy of CAD is percutaneous coronary intervention (PCI). In such a procedure, a peripheral artery is made accessible using an introduction sheath through which a guiding catheter is introduced that is advanced to the ostium of either the left or right coronary artery. A guidewire with a flexible tip is advanced through the guiding catheter and maneuvered distal to the stenosis. The stenosis is, in general, treated by predilation using an expandable balloon followed by stent placement.

MRI perfusion imaging is rapidly developing as a non invasive technique to evaluate perfusion disturbances in the myocardium. Not only is MRI perfusion important for avoiding invasive angiography with negative results but it also delivers information on difference in perfusion between inner and outer layers of the myocardium. This layer specific information is important since especially the inner layer, sub-endocardium, is vulnerable for ischemia because of its proximity to high pressure in the left ventricle when the heart contracts.

Recently, guide wires have been developed equipped with a pressure and/or flow velocity sensor at its tip to obtain intracoronary hemodynamic signals. These signals allow an evaluation of the functional significance of a stenosis resulting in a much better prediction of myocardial ischemia than geometric stenosis evaluation based on angiograms. Moreover, it recently has been demonstrated for one such a physiological parameter, FFR, that when used to decide to treat the stenosis clinical outcome is much better than when decision is guided by angiography alone.

Within WP8 a multi-scale model of the coronary circulation was developed to provide a rational basis for the interpretation of perfusion data and epicardial arterial pressure and flow-velocity information with the goal to identify more accurately patients who would benefit from a revascularisation procedure. A key point of this workpackage was information about the coronary microvascular structure obtained with an imaging cryomicrotome that was used to parameterize a porous-elastic model for modeling perfusion in the myocardium and to validate a new deconvolution approach for quantitative MR perfusion assessment. Furthermore, clinical studies with MRI and measurements of pressure and flow-velocity have been performed to provide data for validation and to propose new diagnostic indices for CAD.

10.1. Coronary microvascular structure

Coronary blood flow is distributed over the walls of the heart by a branching network of large and small arteries which basic characteristics should be captured by a model for myocardial perfusion. Knowledge on these characteristics was obtained by a special designed Imaging Cryomicrotome, ICM, based on spectral episcopic principles. The major coronary arteries of human, pig and dog hearts were cumulated and filled with a fluorescent replica material, not penetrating the capillaries. After freezing the heart it was processed in the ICM, in which it was cut in 20 to 40 micrometer slices in thickness. After each cut the block surface was imaged between 1-7 times at selectable different spectral conditions visualizing the replica and other tracers such as fluorescently labeled microspheres when present for perfusion detection. A highly sensitive camera with 4000 x 4000 pixels was used. In this way a stack of about 4000 images with a total of 64×10^9 voxels was obtained forming a 3D representation of fluorescence in the heart. The vascular structure was extracted applying some specially developed filtering and segmentation techniques. This structure replicates mathematically the vascular structure in vessel segments with known diameter, length and connectivity and allows the automatic detection of blood flow pathways including collateral vessels.

Figure 26 demonstrates the power of ICM to simultaneously detect vascular structure and perfusion distribution by microspheres, which has not been before. The structural information is used for deriving the parameters for the porous elastic model and the microsphere method is used for validating the MRI perfusion technique and predictive power of the model.

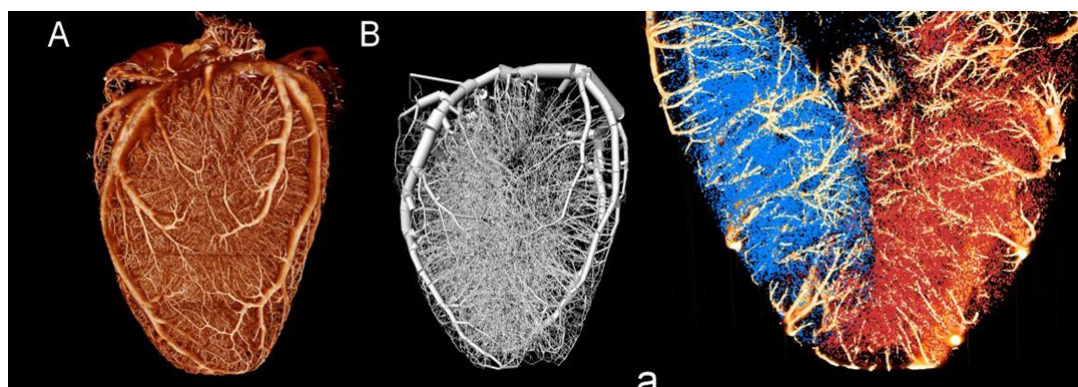


Figure 26 Raw vascular cast data obtained after cryomicrotome analysis of the full tree (left), segmented representation of the raw data down to 50 μm radius vessels (middle) and separation of microsphere colors (right), shown as 3D microsphere distributions for a 10 mm thick slab in the sagittal plane of two canine hearts. Different colors were injected into the LCX and LAD to separate perfusion territories and quantify collateral flow.

10.2. Multiscale multiphysics model for coronary perfusion

Perfusion in the myocardium was modeled as porous media flow governed by Darcy's equation. Figure 27 demonstrates the principle of the porous elastic model. The structure of the blood vessels, specifically their diameter and orientation, is effectively captured by the porosity and permeability tensors which are also dependent on the deformation of the tissue during the course of the heart cycle. Consistency of the discretized Darcy equation as well as

convergence with the correct order have been verified by means of a convergence study for linear and quadratic hexahedral elements.

The interaction between cardiac perfusion and myocardial motion is a well-recognized and physiologically significant phenomenon. To capture the large strain deformation and the complex material behavior, we applied the theory of finite elasticity to model the cardiac tissue. Based on the models of Darcy porous-media flow and finite elasticity we have constructed a coupled fluid-flow elasticity model to describe perfusion in the myocardium. Under the porous-elastic framework it is assumed that fluid and solid constituents co-exist on the same homogenized domain, i.e. there is no explicit geometrical representation of the fluid-solid interface or of the pores.

In parallel, we have pursued the discrete vessel network fluid modeling approach for two reasons. Firstly, rich vascular topological and morphological data is accessible via high resolution imaging modalities, on which to base the design and parameterization of the porous-elastic constitutive model. Secondly, explicit vessel network modeling offers a theoretical means by which to compare and analyze the effects of the ‘smeared’ porous-elastic framework on fluid transport thus achieving a rational micro-macro relationship. In particular, the porous elastic model was validated by the discrete vessel network fluid modeling on the networks from which it was parameterized. The discrete vessel network in turn was validated by microsphere distribution in the same heart from which the networks were extracted.

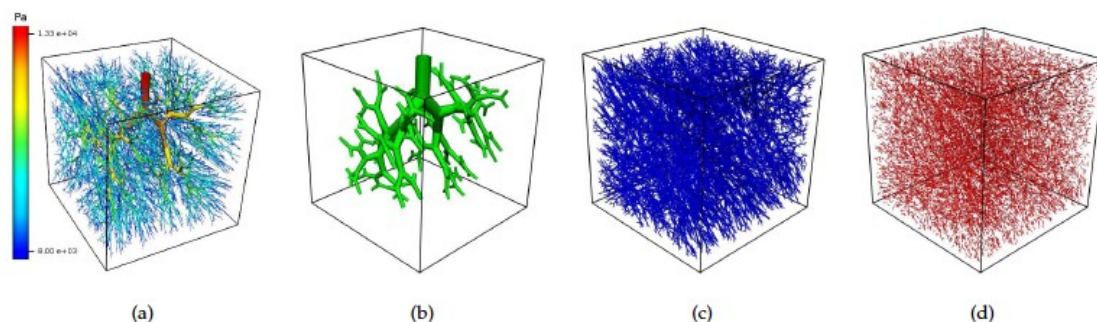


Figure 27 Poiseuille pressure solution for an 8mm cube of tissue (a). Boundary condition pressures of 13.3kPa and 8kPa have been applied at the root node and the remaining terminal nodes resp. The same vasculature is used to parameterise the Darcy model. (b-c) A partition of the vascular model in (a). Mean vessel radii of 30, 6 and 3 micrometers were sought for compartments 1(b), 2(c), and 3(d) resp.

10.3. Clinical MRI perfusion and coronary hemodynamics

Clinical studies applying MRI and measurements of pressure and flow-velocity have been performed to provide material for model validation on the one hand and to derive improved diagnostic tests for CAD on the other hand. To illustrate this work the MRI and hemodynamic measurements obtained nearly simultaneously in MR-CathLab setup at KCL are provided in Figure 28. The hemodynamic measurements were obtained by a guide wire combining pressure and flow-velocity sensors (VOC).

The presented case is interesting since the patient was originally diagnosed angiographically as having three vessel disease and as such a candidate for

bypass surgery. After functional measurements with MR and FFR he was regarded as single vessel disease and treated by PCI. The top panel demonstrates clearly a hypoperfusion of the inferior and lateral wall supplied by the right coronary artery compared to the septum which is most pronounced in the endocardium. Perfusion is normalized after treatment of the stenosis. Ischemia was clearly present from the MRI images but not all physiological indicators derived from the hemodynamic signals agreed with that. This example underlines the need for integral insight of coronary physiology and biophysical principles as can be provided by a comprehensive multi-scale model of the coronary circulation as developed in this workpackage.

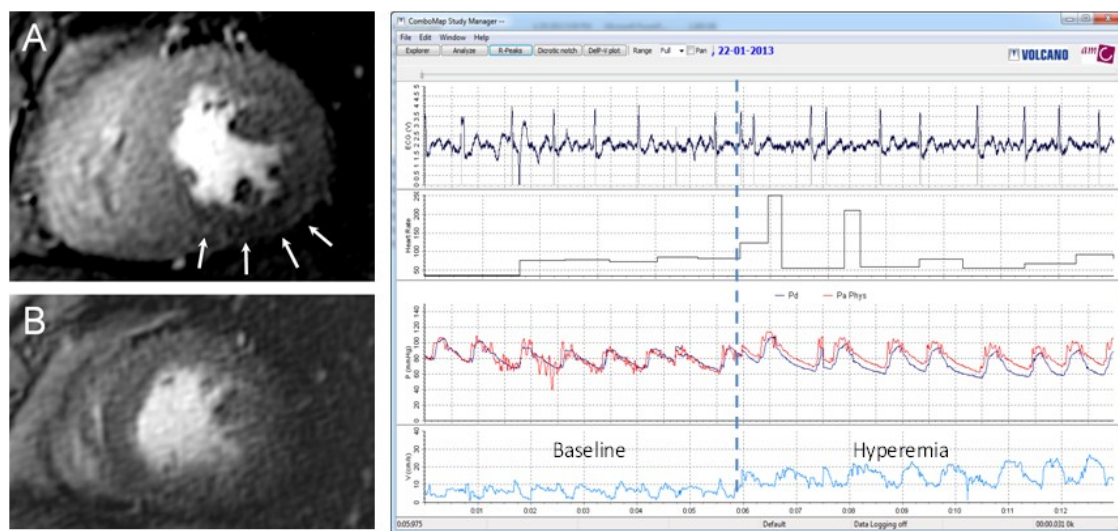


Figure 28 Perfusion MRI of a patient acquired in the MR-CathLab suite at KCL before (top left; the arrows indicate ischemia) and after (bottom left) treatment together with hemodynamic data in the RCA (right). Hemodynamic data comprise from top to bottom ECG, HR, aortic pressure (red) and distal coronary pressure (dark blue) and at the bottom flow-velocity. Note that the pressure drop over the stenosis increase flow increased.

In addition, attention has been paid to alternative indices for stenosis severity without the need for adenosine to obtain maximal hyperemia distal of the stenosis. It could be demonstrated that the ratio between stenosis pressure drop and distal flow-velocity measured at baseline, BSR, had similar predictive strength as FFR. Also the usefulness of the stenosis pressure drop at a flow-velocity of 30 cm/s, Pdv30, was evaluated. Pdv30 was obtained from the pressure flow-velocity relations constructed from sub-maximal vasodilation induced by angiographic contrast medium.

One of the biophysical principles that is often ignored is the effect of cardiac contraction on intramural vessels, the extravascular resistance component. Cardiac coronary interaction can be studied by Wave Intensity Analysis, WIA. Coronary WIA was applied during Valsalva maneuvers in patients undergoing PCI and the extravascular resistance demonstrated. WIA will be an important future validation tool for coronary models.

10.4. Validation of MRI perfusion measurements

MRI perfusion measurements are derived from the pixel wise analysis of contrast passing through the myocardium. Such passage curves can be translated into local flow. A constrained deconvolution approach using a Fermi function model was developed to derive quantitative perfusion values from MRI. The method was validated by a mock circulation system and resulted in excellent correlations between MRI and model flow. The method was also evaluated using isolated slaughterhouse pig hearts and fluorescently labeled microspheres. By accounting for the disproportionate microsphere distribution at bifurcating segments with the largest branch angles, ranging from 100° - 120° , reduced the error from 24% to 7% in between the fraction of flow predicted by the 1-D Poiseuille model and the fraction of microspheres.

10.5. Model for whole heart perfusion

The model for whole heart perfusion couples the structure of the epicardial arteries as derived from MRI images with the porous elastic model for the myocardium. In this way perfusion defects can be simulated demonstrated in Figure 29. With this result, the workpackage laid the foundation for the interpretation of MRI images as presented in Figure 28 in terms of distribution of biophysical parameters such as porosity and contraction patterns.

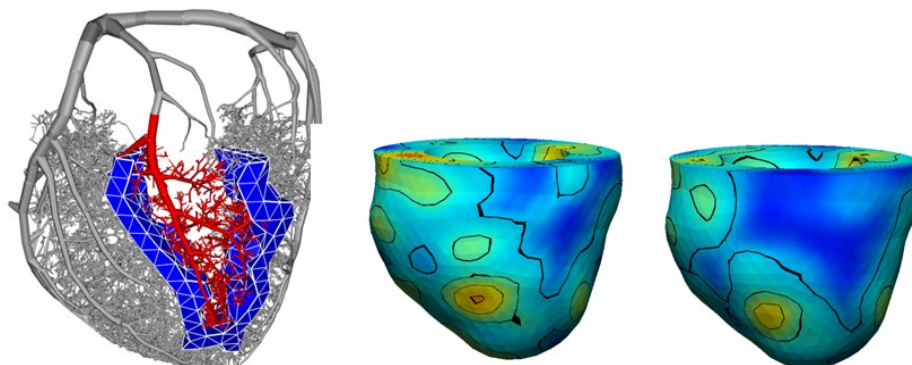


Figure 29 The cross-sectional area of the feeding artery of the red subtree (left) was decreased by a factor of 0.7 to model stenosis of a branch of coronary artery. MRI perfusion imaging (middle: without stenosis; right: with stenosis) was simulated as the contrast agent concentration in the tissue 20 seconds after administering a bolus injection.

11. WP9 - Valvular and Aortic Disease

This work package is concerned with blood flow in the aorta, which is the first artery in the systemic circulation carrying the blood away from the left ventricle towards most of the organs of the body. Any change in aortic impedance (afterload) can have significant physiological implications on the heart itself. In particular three different aortic diseases are considered, aortic coarctation, aortic dissection and aortic valve stenosis.

Coarctation of the aorta is typically a discrete stenosis of the proximal thoracic aorta that restricts the left ventricular blood outflow to the body. It is the fourth most common lesion requiring cardiac catheterization or surgery during the first year of life and has a significant impact in terms of mortality, morbidity and allied healthcare costs. Coarctation varies considerably in its anatomy, physiology, clinical presentation, treatment options, and outcomes. Treatment criteria rely on clinical investigations such as echocardiography, MRI and catheterization. In particular, the pressure gradient across the coarctation is an important measure. Coarctation diagnosis and treatment would benefit from an approach to measure this quantity non-invasively and ultimately without the pharmacological inducement of a stress condition.

Dissection of the aorta is defined by the splitting or delamination of the layers of tissue that make up the aortic wall. Within these three layers – the intima, media and adventitia – dissections can occur at a range of depths, either between layers or within the media. Aortic dissection has an estimated incidence of 2 in 10,000. The prognosis of patients with an acute dissection is poor with overall mortality rates of 6- 39%, and even up to 58% for non-operated patients. Current patient management is based on the patient's symptoms, their general condition (age, co morbidities etc.) and on imaging (mainly morphological) information available from CT and MRI. Supporting diagnostic information including hemodynamic measures from blood flow simulations that are not available by direct clinical measurement are believed to provide important insights for coarctation diagnosis and treatment.

Acquired aortic valve stenosis – a condition where the aortic valve does not open properly anymore - is present in 30% of individuals older than 65 years, and in nearly 40% of individuals older than 75 years. It results in an increase in left ventricular afterload and decrease in systemic and coronary flows as consequences of valve obstructions. The appearance of symptoms such as angina is associated with an average survival of only 5 years. The primary management of symptomatic patients is surgical intervention. The timing of intervention is determined by the severity of the stenosis and the presence of symptoms. Diagnostic studies include CT, MRI, echocardiography and stress testing. Invasive cardiac catheterization may be required if clinical findings are not consistent with echocardiogram results. Predicting the patient-specific hemodynamic response under stress conditions might support diagnosis and treatment, and simulating the pressure distribution across the aortic valve might avoid invasive tests.

Within this work package, system models that are able to represent the afterload on the heart, and thus to support the modeling of the heart and vasculature as an integrated system were revisited. In addition, computational work flows were developed to enable the use of blood flow simulations in the process of diagnosis and treatment of aortic coarctation, aortic dissection and aortic valve stenosis. These computational work flows were applied to cases and evaluated in clinical centers

11.1. Circulation and anatomical models for public access

A major review (181 references) of published circulation models was undertaken, leading to a publication in an open access journal, Biomedical Engineering Online. This review article, published in April 2011, is highly accessed: it was the eleventh most accessed of all articles in this journal in the twelve month period leading up to the euHeart General Assembly in October 2012, with 5421 accesses in that period. Following the review of available models a family of relatively simple zero-dimensional circulation models was developed in the CellML Markup language and published in the CellML model repository for open and public access.

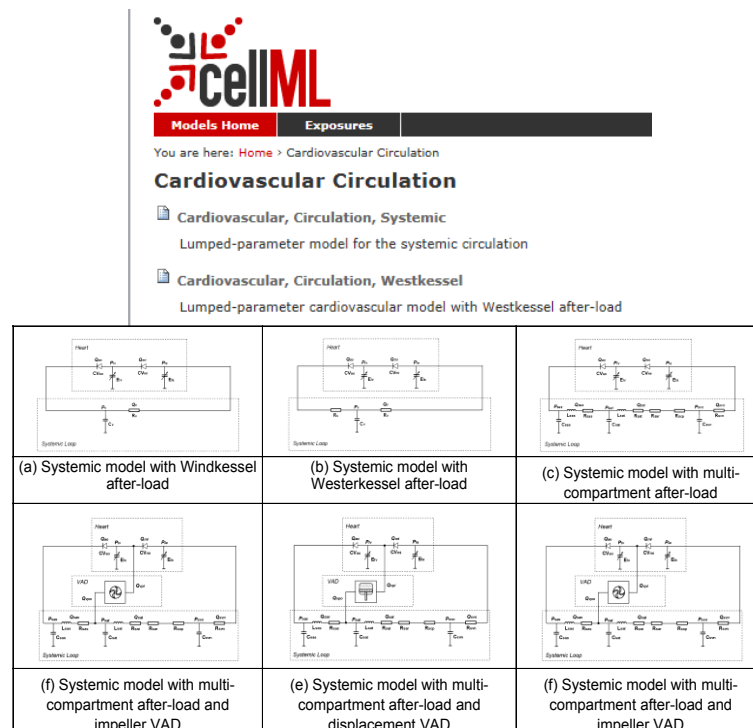


Figure 30 Illustration of some of the circulation models encoded in CellML and available via the model repository.

11.2. Work flows for aortic and valvular disease

Computational work flows were developed for the assessment of hemodynamics using patient-specific anatomies for the three target diseases. Each of these work flows is complete in itself and assembled from a series of components. The fundamental processes are the same for each work flow (see

Figure 31 for the aortic dissection work flow), but different components were used because of application-specific requirements and preferences of the consortium members doing the actual development.

The work flow starts with the loading of a medical image. This is segmented to identify the region of interest for which the hemodynamics will be computed. Each of the three work flows chose a variation of an image registration algorithm to achieve the segmentation. For the valve application it was based on the morphing of a parametric model to the patient image. For the aorta applications, because of the wide variation in the individual anatomy in terms of the detailed configuration of the branching structure at the supra-aortic vessels and of the aortic dissection, a novel algorithm was developed to perform a series of registration to grow the aorta from a seed region. Typical segmentation results for the three applications are illustrated in Figure 32.

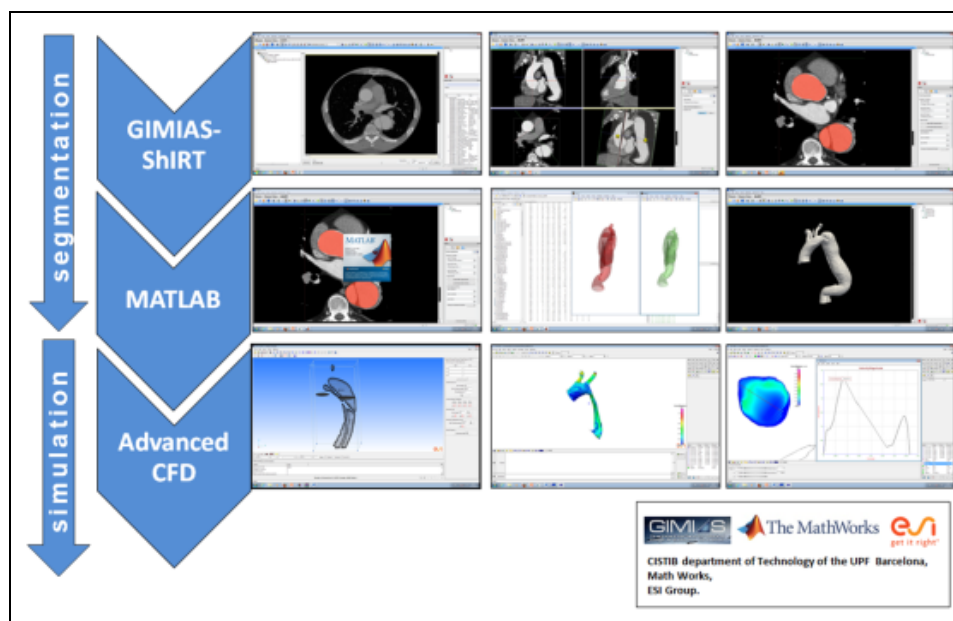


Figure 31 Diagram of the computational work flow for the aortic dissection application.

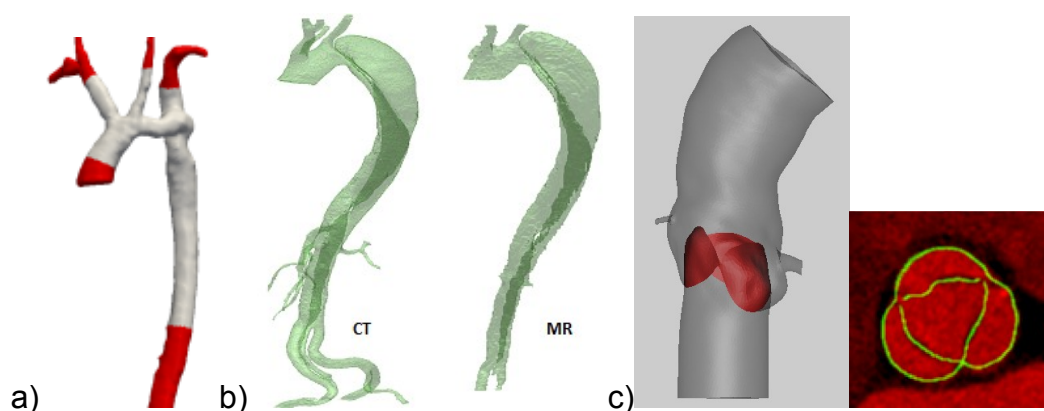


Figure 32 Sample segmentation results for aortic coarctation (a), aortic dissection (b) and aortic valve (c).

The next step is to set the boundary conditions that determine the pressure or flow conditions at the inlets and outlets of the detailed anatomical region to be studied. These might be explicit conditions based on clinical measurements in the individual or they might themselves be models such as the circulation models described previously. In some cases pressures are available from direct measurement using catheters in the aorta of the patient. Similarly in some cases the flows at boundaries have been measured have been measured using either ultrasound or phase-contrast magnetic resonance imaging. The work flows include tools to interpret the images of flow for use as boundary conditions for the computational fluid dynamics analyses.

Afterwards the material properties are specified and then the computational analysis is performed. The simplest analyses assume that the boundaries of the anatomical structure, in this case the vessel wall, are rigid and compute the fluid dynamics (the distribution of pressure and velocity, together with a number of derived parameters such as wall shear stress) within it when subjected to the specified boundary conditions. In more sophisticated analyses Solid Interaction (FSI) approaches are used. The wall is considered to be deformable and additional equations, with appropriate coupling to the fluid mechanics, are solved to compute the displacements and stresses and strains within it. Figure 33 shows some sample results.

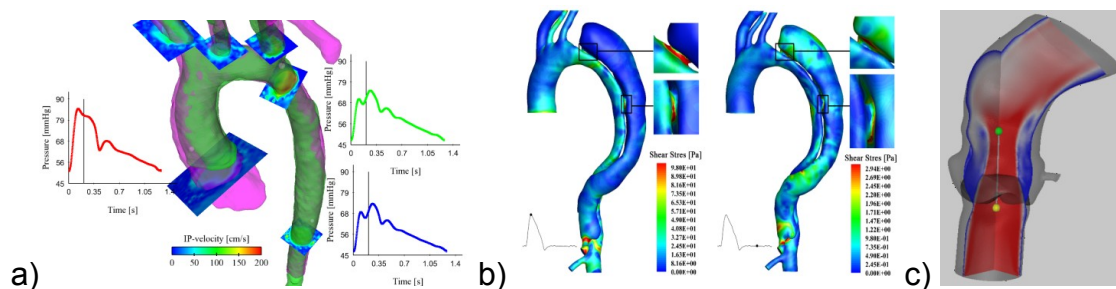


Figure 33 Analysis results for aortic coarctation (a), aortic dissection (b), and aortic valve stenosis (c).

Building the computational workflows involved the development of a number of novel methods:

- The aorta segmentation methods developed in work package WP3 have been applied both to produce physically-plausible time-series segmentations of the aorta and, integrated with the segmentation process, to estimate the distribution of stiffness within the aorta.
- For the aorta a compressible flow analogy based on the one-dimensional wave equation has been shown to capture, at low computational cost and at least to a first approximation, the wave transmission effects associated with the dilation of the vessel.
- A method of analysis of valve dynamics has been developed that does not require the full sophisticated fluid-solid interaction (FSI) analysis, and it has been shown that the resulting flow patterns are very similar to those from FSI.

- In collaboration with work package WP4, the data assimilation methods have been applied to vascular structures (both idealized and real) and it has been shown that local stiffness parameters can be recovered directly as part of the FSI analysis process by assimilating information from the segmented images.
- For the dissection application, a novel and efficient method to represent the interactions between the graft and the vessel wall during the deployment process has been developed, to support the rapid virtual deployment of a stent graft, in the individual patient anatomy, to predict the effects of candidate interventions.

11.3. Evaluation of work flows in clinical centers

The specifications for the work flows and the final evaluations were provided and performed by the clinical partners at KCL and UHD. The preparation time for a new case was typically between one and two hours for an experienced operator for each of the work flows. This has been achieved by automating as many steps in the process as possible. The work flow that requires most user intervention is that for aortic dissection. Run times depend on the application and on the available computational resource, but are of the order of hours or days.

The aortic coarctation work flow was operated on sixteen clinical cases, as well as on a number of healthy controls. The primary target was to produce computationally measures of the pressure gradient across the coarctation without using invasive measurements. The aim is that this would be operable on every patient using only image and external cuff pressure data. The final correlation achieved within the lifetime of the project for the relationship between computed and measured mean pressure gradients is shown in Figure 34.

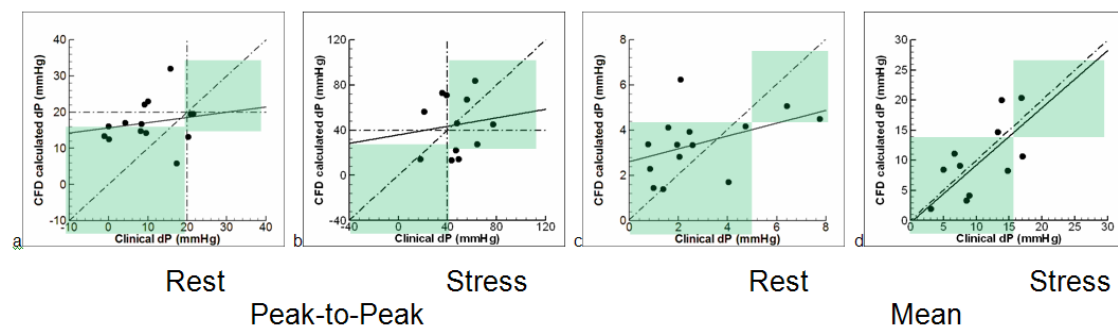


Figure 34 Comparison of measured versus computed pressure gradient for sixteen aortic coarctation cases: where cases fall within green rectangles the diagnosis would be the same as for invasive measurements.

A précis of the final coarctation work flow evaluation report by the clinical partner at KCL follows:

“The aortic coarctation analysis workflow clearly shows its feasibility and clinically-friendly user interface, showing that it could be incorporated in the clinical centers. From our point of view, a great effort has been made to bring different software packages together and to create a smooth and easy to follow

tool-chain for processing. The training required for a clinician to learn how to perform a complete simulation can be achieved in a reasonable time. The manual provided to follow the tool chain is comprehensive, well written and very logical. If the manual is strictly followed step by step, the simulation can be performed without any problems. Preparing a simulation requires less than two hours and after being trained running several simulations, they can be prepared in about one hour, which is a very efficient time. On the other hand, we feel that there are a few minor changes that could be added to improve the software and make it more clinically-friendly. It would make easier its incorporation into the clinical environment. Overall we are very satisfied with the operation of the software work flow. The primary limitations are that the quantitative accuracy of the simulations on a case-by-case basis is probably not yet sufficient to support the replacement of the invasive clinical investigation by its computational counterpart, and that an optimal process would include extrapolation from the rest to the stress condition without the need for the pharmacological intervention.”

The dissection work flow segmentation was operated on ten cases, and that for the aortic valve analysis was operated on nine cases. Quantitative comparisons of ‘gold-standard’ manual and automatic segmentations provided by the work flows were reported, with satisfactory results in both cases. For the valve work flow further validation was performed using an experimental phantom. Generally the final conclusions were the same as those for the coarctation work flow. For all applications it has been recognised that some further improvements in robustness, fault-tolerance and ease-of-use are required before the work flows can be exposed with confidence to a cohort of users with more variable levels of expertise.

12. WP 10 – Clinical Data Acquisition and Validation

The overall goal of WP10 was to specify the clinical requirements of the euHeart studies, which define the role of the suitable biophysical models, and the required clinical data acquisition and metrics. Furthermore, advanced data acquisition protocols (like free breathing whole heart volume MRI and 4D morphology, motion and perfusion) have been developed and evaluated. In addition, a simulator for the pre-operative rehearsal of RFA interventions using personalized cardiac-electrophysiology simulations was developed to underpin the dissemination of the biophysical models to the medical community.

12.1. Free breathing cardiac MRI with advanced motion compensation

A real-time 2D navigator using startup profiles of SSFP sequences has been developed. In a retrospective application scenario, all images are reconstructed and the motion correction is preformed offline (Henningsson M., et al., Magn Reson Med, 2012. 67 (2): 437-445). Figure 35 shows that the 2D navigator (2DSN) improves image quality compared to the diaphragmatic 1D navigator in healthy subjects. For prospective application, the 2D navigator relies on image reconstruction and registration in real-time. This prospective 2D navigator is better than the 1D navigator for very large gating windows (see Figure 36 for sample images). However, more efficient reconstruction and registration algorithms are needed for multiple coil reconstruction and affine registration in real-time.

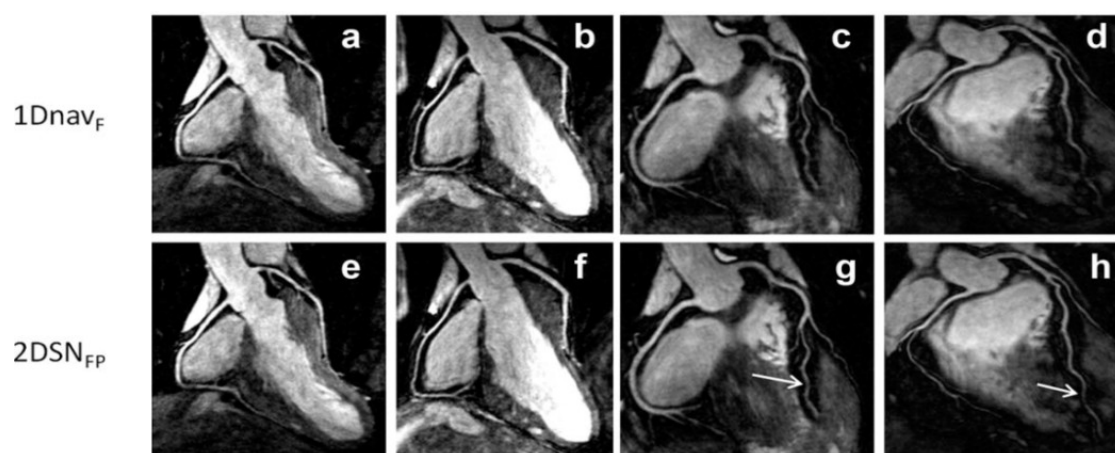


Figure 35 Exemplary images obtained with a 1D and a 2D navigator for motion compensation. Motion correction was performed offline.

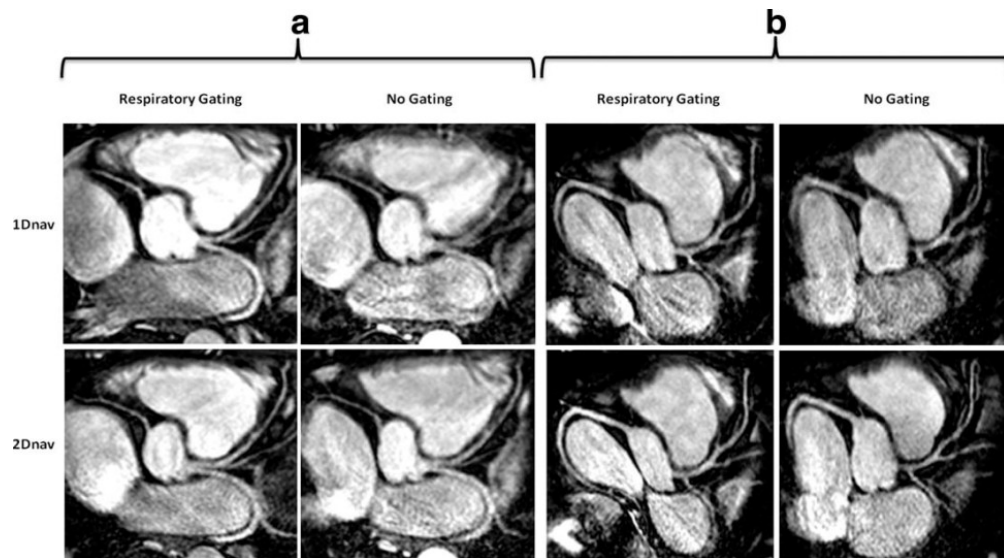


Figure 36 Exemplary images obtained with a 1D and a 2D navigator for motion compensation. Motion correction was performed during acquisition.

12.2. Highly accelerated and accurate MR flow

The two main aims for the 4D MR flow work were (i) to improve the accuracy of MR-flow and (ii) to accelerate the acquisition of MR-flow. Improving the accuracy of MR flow has been achieved by using a magnetic field camera. This camera can remove background phases using a pre-calibration scan and is independent of the scanned object. Compared to image based correction methods, the magnetic field camera can also successfully be applied in scans without static tissue (Giese D., et al., Magn Reson Med, 2012. 67(5): 1294-1302). Accelerating the acquisition of MR-flow has also been achieved by improving kt-PCA. This has been done by sparsifying temporal support and excluding physiological 'impossible' temporal behaviors. A net acceleration rate of 8 has been shown to be feasible in 2D PC-MRI.

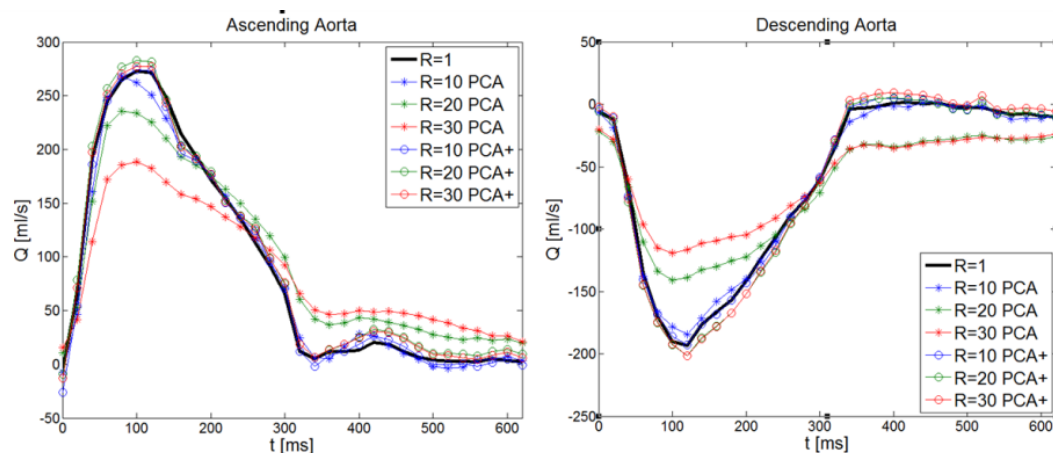


Figure 37 Accelerated MR flow in ascending and descending aorta (R = nominal acceleration factor; PCA = kt-PCA, PCA+ = compartment-based kt-PCA).

12.3. Flow quantification from 3D Doppler ultrasound

The two main aims of the 3D color Doppler ultrasound work were (i) to produce 4D flow fields and (ii) to obtain accurate flow quantification. 4D flow fields were constructed by combining multiple 3D color Doppler images acquired from 3 or more views. The images were registered and the resulting velocity field is obtained by fitting the registered input images into a 3-dimensional B-spline grid. The fitting is regularized by penalizing the divergence of the reconstructing vector field, which should be incompressible. The temporal resolution was increased by interleaving trigger-delayed echo Doppler sequences. Figure 38 compares flow rates obtained from multi-view 3D color Doppler with results from phase contrast MR.

The standard methods for flow quantification from color Doppler is angle dependent and assumes a circular section which produces an inaccuracy of >30% error. Our proposed approach of flow quantification from temporally interleaved multi-view 3D color Doppler is angle independent. The time-resolved flow rate curves may be computed by interleaving delayed sequences; therefore combining multiple views may increase coverage.

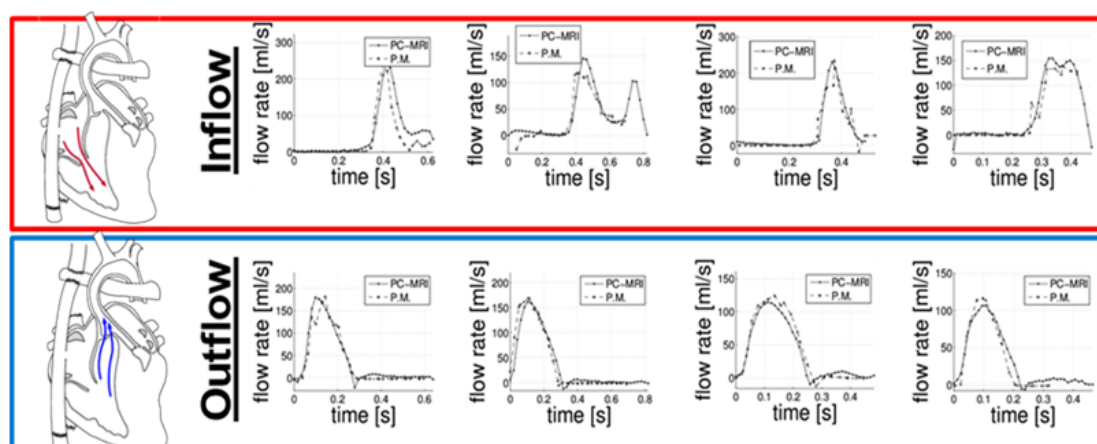


Figure 38 Comparison of flow measurements from multi-view 3D color Doppler with results from phase contrast MR for four HLHS patients. Outflow refers to the blood flow (flow rate and volume per cycle) through the neo aorta. Inflow refers to the flow (flow rate and volume per cycle) through the tricuspid valve.

12.4. Curvilinear analysis and approximation of cardiac DTI *in-vivo*

Aims of the *in vivo* cardiac diffusion tensor imaging were to (i) develop a dedicated analysis technique for the ventricle shape and (ii) to have a description of fiber orientation of the full ventricle. Image acquisition was split into two parts, firstly the acquisition had to be adapted in order to cope with cardiac motion and then retrospective motion correction was applied to produce tensor reconstructions. As DTI acquisition is limited with high background noise, a dense approximation of the entire LV fiber architecture was required. For that purposed, the DTI data were transformed, an anisotropic kernel approximation was computed and the dense tensor field was warped back in LV anatomical reference space. The cardiac DTI acquisition method was applied *in vivo* in diastole and systole (see Figure 39) and good correlation with previously reported *ex-vivo* studies was achieved. Dual-phase curvilinear analysis shows,

for the first time, dynamics of the fiber architecture in vivo. The dense approximation allowed for fiber tracking, leading to the depiction of a helical structure in both phases in vivo.

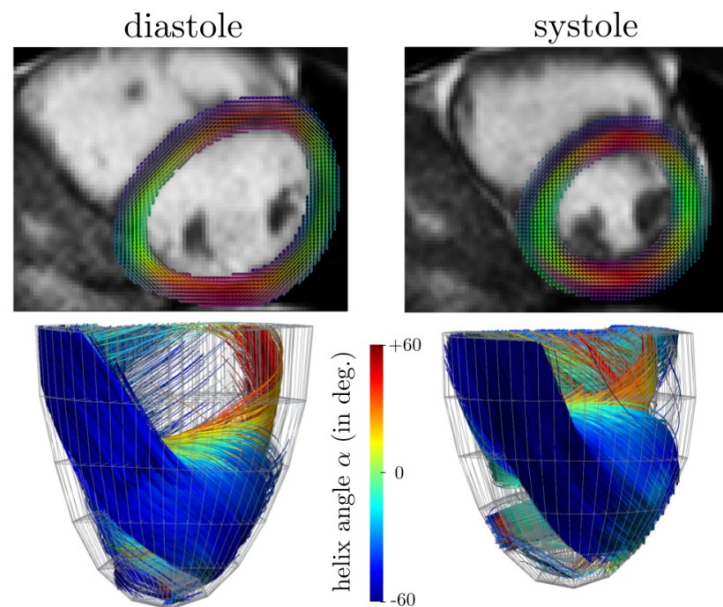


Figure 39 Muscle fibre structure in the left ventricle as obtained with the cardiac DTI acquisition method.

12.5. Endovascular simulator for radiofrequency ablation

Despite the wide adoption of radio-frequency ablation therapy throughout the western world, this therapy remains challenging due to difficulty to navigate inside the cardiovascular system with X-ray guidance and to interpret the various electrophysiology signals measured during the intervention. In addition to improving the planning of radiofrequency ablation procedures for AF and VT as described in WP6, we have developed an endovascular simulator which aims at training electrophysiologists to perform cardiac radiofrequency ablation procedures, in particular for VT cases. Compared to existing endovascular simulators, our approach is based on the real-time biophysical simulation of electrophysiology and on patient specific datasets. The simulator uses a specific hardware which can track guidewires and catheters and simulates the visualization of X-ray during the endovascular navigation and the visualization of electrophysiology signals measured inside the ventricles. The current version of the prototype allows the user to simulate the action of pacing leads and radiofrequency ablation catheters.

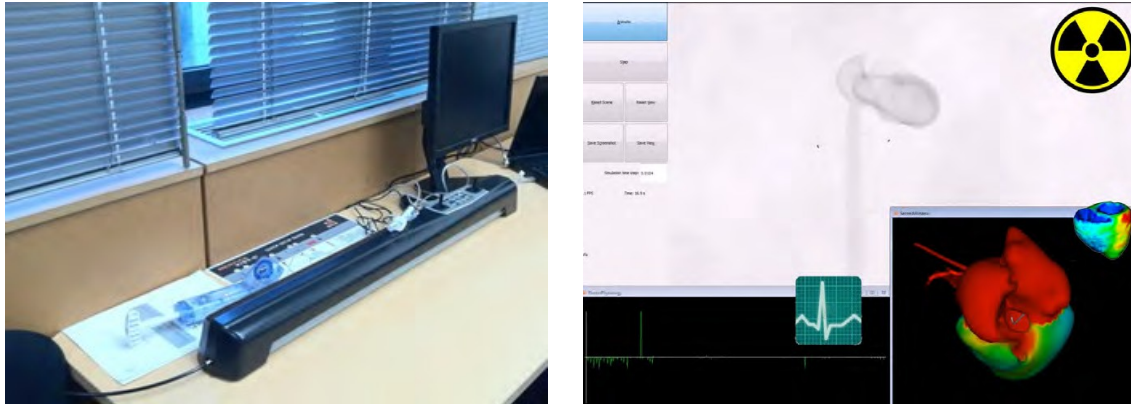


Figure 40 View of the force-feedback device used to track catheters and guidewires during endovascular simulation (left) and view of the 3 windows of the simulator: the X-Ray view, the display of electrophysiology signals and a 3D view of the scene (right).

13. Conclusions

Starting from the modeling knowledge available in the consortium at the beginning of the euHeart project, methods for personalizing cardiac simulations for the 5 major disease respective treatment areas of cardiac resynchronization therapy, radiofrequency ablation, heart failure, coronary artery disease and aortic and valvular disease have been developed to improve diagnosis, treatment planning and delivery, and optimization of implantable devices. To fully exploit the complementary expertise in the consortium and enable sharing of the results with the wider VPH community, a web-based database (AMDB) has been developed, populated with models from the consortium, and extended with computing services (HeartGen) facilitating building of models. In addition, the modeling descriptions CellML and FieldML have been further developed to provide and establish a standard that makes models and simulation approaches sustainable as other groups can reuse and build upon previous results in their future work.

Two enabling technologies that are essential for personalizing heart models and cardiac simulations have been advanced. First, the analysis of biomedical images plays a fundamental role as these images provide information about the individual heart anatomy and motion as well as a wealth of disease related information. Methods have been developed that allow for the efficient generation of patient-specific anatomical models from medical images of multiple imaging modalities. These models, for instance, account for myocardial deformation, cardiac wall motion, and patient-specific tissue information like myocardial scar location. The second technology addresses personalization of model parameters that are not directly observable from available clinical data but play a key mechanistic role in the disease process. Examples cover, for instance, the contractility of the cells in the myocardium or the material properties of the aortic wall. To address this task the assimilation framework Verdandi has been developed that assimilates observations into a model by acting on the discrepancy between the measurements and the values derived from the computational model across scales (e.g. protein level ion channels flux and whole organ deformation) and functions (e.g. mechanical contraction and electrical activation).

Adaptation of the models and simulation approaches for the 5 disease areas considered in euHeart resulted in a wealth of new approaches, technical improvements and insights. Approaches to enrich models with information that is essential for simulations, but cannot be directly derived from available medical images such as the muscle fibre directions in the myocardium or fast the conduction tracts of the heart have been developed. Numerical fluid-structure simulations have been improved to be able to simulate a heart with LVAD support, including contact of the cannula with the ventricular wall. Information about the coronary microvascular structure has been derived from human, pig and dog hearts using an imaging cryomicrotome and used to parameterize and validate a porous-elastic perfusion model. The simulations have been integrated into prototypes together with associated tools to enable application in a clinical context and clinical validation. Specific examples are the

CRT planning environment, the work flows for fluid-dynamics based analysis of aortic and aortic valve disease and the simulator for radiofrequency ablation. The models, simulations and prototypes were focused on clinical questions in relation to the 5 disease areas with the goal to improve patient selection, to improve procedure planning, to develop approaches that replace invasive measurements by non-invasive surrogates, and to tune implanted devices on a personalized basis.

To provide data for model development, to show the benefit of the developed models and to quantify their clinical benefit, the work in euHeart was from the beginning accompanied by clinical data acquisition activities complemented by work on innovative acquisition techniques, for instance for 4D flow and in-vivo imaging of the muscle fibres in the heart. Part of these data sets comprised data for model building as well as specific (invasive) acquisitions to enable model validation. These data allowed demonstrating that, for instance, a personalized electromechanical model of the left and right ventricular myocardium is able to predict the acute response to CRT for two patient cases. Image-derived measurements of the pressure gradient across aortic coarctations showed the potential of the approach, though further improvements are required. Models and simulations have also been used to derive new clinical indices. For example, simulations of anatomy and diastolic filling in systemic right ventricular patients allowed deriving a new metric to assess diastolic function in these patients. Finally, new clinical indices exploiting image and data analysis have been proposed and evaluated for patient selection in CRT from US images and assessment of stenosis severity from pressure and flow measurements in the coronaries.

In summary, proven by more than 300 publications of which 128 have been published in peer-reviewed journals, the euHeart project significantly advanced the state-of the-art in cardiac simulations. The project demonstrated the predictive value and clinical potential of personalized cardiac simulations for several clinically relevant settings. Setting up personalized models and simulations was very time consuming limiting their application to a small number of patient cases during the euHeart project. Clinical validation for a large number of patient cases is intended to be done in future projects.

14. Impact

The impact of the euHeart project is threefold. First, the results allow improving healthcare in the area of heart disease that is a highly relevant and epidemiologically significant contributor to loss of quality and quantity of life within Europe. Second, the results allow innovating medical devices. Finally, the euHeart made a significant contribution to the VPH community and vision.

14.1 Contribution to better healthcare

Diagnosis – The use of personalized biophysical simulations enriches clinical practice by providing patient-specific physiological information about the heart which is either currently not available such as the contractility of the left ventricular myocardial tissue or becomes available via non-invasive measurements like image-derived measurements of the pressure gradient across an aortic coarctation. In addition, results generated by the simulation frameworks provide the clinicians with a better understanding of the pathologic mechanisms and enable prediction of disease progression as shown by the simulations of anatomy and diastolic filling in systemic right ventricular patients. Furthermore, euHeart results contribute to the understanding and consistent interpretation of the various fragmented and inhomogeneous data generated by current diagnostic systems.

Therapy Planning and Guidance – euHeart results help with selecting the proper treatment by providing new clinical indices correlating with CRT response and stenosis severity. Most importantly, euHeart demonstrated the feasibility of in-silico therapy planning and a personalized electromechanical model of the left and right ventricular myocardium was shown to predict the acute response to CRT for two patient cases. In addition, it was shown for two patient cases that VT can be simulated in-silico leading to similar re-entry patterns as observed with invasive measurements. Both examples demonstrate the great potential to facilitate therapy planning with the simulation environments. In a further step, the optimised interventional plans can be integrated into image guided interventional systems that are increasingly being used for treatment delivery in CVD to improve treatment delivery and increase the safety of care. More specifically, target points for pacemaker leads or ablation lines resulting RFA planning can be merged with the interventional images and displayed to the clinician. Combining optimised interventional plans with guidance systems has the potential to reduce the dependency of the treatment outcome on the clinician's experience and ensures better reproducibility of the intervention.

Training – Exact and efficient pre-operative planning and rehearsal is an important factor for a good outcome in patient's treatment. Like in every profession that demands cognitive capabilities coupled with manual skills, an optimal preparation to complete a challenging task successfully is important. The simulation results from the work on electrophysiological modeling have been integrated into a prototype simulator for radiofrequency ablation. Unlike state-of-the-art simulators which are only available with precalculated non-individual human models for training purposes, our simulation prototype is

based on the real-time biophysical simulation of electrophysiology and on patient specific datasets to present a highly individualized simulation surrounding, needed for efficient pre-operative planning and rehearsal.

14.2 Medical device innovation

Imaging devices and IT – Within the euHeart project, several new acquisition protocols and a wealth of image analysis methods have been developed. Examples are protocols for 4D MR flow imaging and enhanced analysis methods that make, for instance, MR perfusion imaging quantitative or allow quantification of motion abnormality. Imaging devices and clinical workstations benefit in the short term from these results. At the same time, these results pave the way from a purely descriptive data interpretation towards in-silico disease quantification and prediction of disease progression. They build the basis of a new generation of products exploiting bio-physical simulations for data interpretation and therapy planning with their numerous benefits for better diagnosis, therapy planning, guidance and treatment rehearsal.

Implantable and interventional devices – The design of implantable devices such as artificial valves or LVADs can be optimized using the simulation tools developed within the euHeart project making the development process much more effective. Moreover, the simulation environments allow to access values which are not able to be measured directly or only in interventional conditions. This additional information that becomes available via the simulation techniques makes it also possible to optimize device implantation. Results showed, for instance, that the ascending aorta is the most advantageous gross location for the outflow cannula of an LVAD device. Furthermore, new indices and approaches for assessing coronary stenosis severity will influence the analysis of data obtained from catheter equipped with pressure and flow sensors.

14.3 Contribution to the VPH












From the beginning, the euHeart project is consistent with the philosophy of the VPH community with the goals to verify and validate developed models, to enable patient-specific simulations reflecting normal and pathological conditions and to provide integral access to clinical users to promote the acceptance of and engagement with the VPH vision by this community. Core members of the consortium have been involved in or leading other projects such as VPH-Share. Next to more than 300 publications resulting from the euHeart project that document and promote not only project results, but also demonstrate advances towards the VPH vision, a number of key results have been made available to the VPH community in particular. These comprise, for instance:

- The model database AMDB complemented with the HeartGen service that supports the generation of personalized simulation models. This database has been populated with models resulting from the euHeart project.
- Advances of the modeling standards FieldML and CellML and the related visualization tool cmgui. In addition, a family of simple zero-dimensional circulation models was developed in the CellML language and published in the CellML model repository for open and public access.

- The assimilation library Verdandi for the personalization of model parameters that are not directly observable from available clinical data but play a key mechanistic role in the disease process.

Next to demonstrating feasibility of the VPH vision towards industrial participants and clinicians, and initiating commercialization of VPH technology at multiple levels, euHeart provided sustainable key contributions on which future work of the VPH community can build upon.

15. Contact Information

Beneficiary name	Beneficiary short name	Logo
Philips Technologie GmbH (Jürgen Weese, juergen.weese@philips.com)	PRA	
The University of Oxford (Peter Hunter, p.hunter@auckland.ac.nz)	UOXF	
Universitat Pompeu Fabra (Alejandro F. Frangi, a.frangi@sheffield.ac.uk)	UPF	
The University of Sheffield (Rod Hose, d.r.hose@sheffield.ac.uk)	USFD	
Institut National de Recherche en Informatique et Automatique - France (Herve Delingette, Herve.Delingette@inria.fr and Dominique Chapelle, dominique.chapelle@inria.fr)	INRIA	
King's College London (Nicolas Smith, nicolas.smith@kcl.ac.uk Reza Razavi, reza.razavi@kcl.ac.uk)	KCL	
Academic Medical Center Amsterdam (Jos Spaan, j.a.spaan@amc.uva.nl)	AMC	
Karlsruher Institut für Technologie (Olaf Dössel, olaf.doessel@kit.edu)	IBT	
Institut National de la Santé et de la Recherche Médicale (Mireille Garreau, Mireille.Garreau@univ-rennes1.fr)	INSERM	
Philips Healthcare (Marcel Breeuwer, marcel.breeuwer@philips.com)	PMS	
Berlin Heart GmbH (Peter Nüsser, nuesser@berlinheart.de)	BH	

HemoLab BV (Jurgen de Hart, j.dehart@hemolab.nl)	HL	HemoLab cardiovascular engineering
Universitätsklinikum Heidelberg (Hendrik von Tengg-Kobligk, Hendrik.Tengg-Kobligk@med.uni-heidelberg.de)	DKFZ	 UniversitätsKlinikum Heidelberg
Volcano Europe SA / NV (Angela Richter, arichter@volcanocorp.com)	VCO	
Servicio Madrileño de la Salud (Julián Pérez-Villacastín, jvillacastin@secardiologia.es)	HSCM	 SaludMadrid
Philips Ibérica S.A. (Javier Sánchez Gonzalez, javier.sanchez.gonzalez@philips.com)	PMSI	PHILIPS